Author version: *Geomorphology, vol.214; 2014; 436–451*

Coastal processes and longshore sediment transport along Kundapura coast, central west coast of India

Shanas P.R., Sanil Kumar V*

CSIR-National Institute of Oceanography (Council of Scientific & Industrial Research), Dona Paula, Goa - 403 004 India

*Corresponding author: Tel: 0091 832 2450 327 Fax: 0091 832 2450 602 Email: sanil@nio.org

Abstract

Longshore sediment transport (LST) is one of the main factors influencing coastal geomorphology. This study examines the variation in the LST estimate using four well known formulae and the sensitivity of wave parameters on LST determination. The study was done along the Kundapura coast, central west coast of India. The Delft3D-wave module was used for obtaining the nearshore wave characteristics from the wave data measured using Datawell directional wave rider buoy at 12 m water depth for a period of one year. Diurnal change and seasonal variation in LST were examined. The study shows that the net LST was towards north for most of the time (non-monsoon period) during the year when predominant wave direction was between SWS and SW, whereas the LST was towards south during the monsoon season when the wave direction was from the west**.** It was found that the influence of breaker height was more during the non-monsoon period whereas during the monsoon period, breaker angle shows more influence on LST. Estimated annual net LSTR for the region is 3.6, 3.0, 1.6, and 2.6 x 10^5 m^3 based on the CERC, Walton and Bruno, Kamphuis and Komar formulae. The LSTR estimate based on the Kamphuis formula, which also includes the wave period, beach slope, and sediment grain size, was found to be a reliable estimate for the study region. The variation in LSTR estimate considering different data intervals was also examined and found that the difference in monthly LSTR for data intervals of 6, 12 and 24 h with respect to the 3 h interval was up to 11, 13 and 24%. For better and more accurate estimates of LSTR, the data interval should be 3 h or less.

Key words: Longshore currents, sediment transport, nearshore waves, nearshore processes, littoral drift

1. Introduction

The coastal environment constitutes a fragile and complex ecosystem that is an important resource for most nations. The littoral drift or longshore sediment transport (LST) is one of the main factors influencing the coastal geomorphology (CERC, 1984). A quantitative understanding and thorough knowledge of LST in the littoral zone is essential for the design of coastal protection measures and operational maintenance of navigation channels. In the normal course, if some beach material is washed away during a rough weather season, the lost material is re-deposited during the next fair weather season and the beach equilibrium is maintained (Komar, 1998). However, when there is an obstruction to littoral drift due to the presence of natural headlands, shoals and/or artificial structures, the equilibrium profile of the natural beach is disturbed (Komar, 1998). Quantitative prediction of coastal processes and coastal evolution through numerical modeling is now possible due to the major advances that have been made in understanding the physical processes and mathematical modeling techniques over the last few years (e.g. Jiang et al., 2010). Because of the complexity of the nearshore processes, accurate estimation of longshore sediment transport rate (LSTR) is still a task for the coastal engineers (Mafi et al., 2013). The accuracy of the prediction depends on the environmental conditions at the nearshore zone, the governing physical processes, and the quality of the data used to calibrate the formulation (Güner et al., 2013).

Generally there are two fundamental approaches for the estimation of LSTR. One is with the bulk formulation which is based on the assumption of simplified physical processes and the other one is the process-based models which include the effects of large number of complex physical processes. The process-based models require a large number of input parameters (Mil-Homens, 2012). In the surf zone of sandy beaches, the LSTR is controlled by the waves through wave breaking and wave-induced currents (Van Rijn, 2002) and hence are mainly related to breaking wave parameters. So the bulk formulation requires wave characteristics in the breaker zone. Also, due to the difficulty of acquiring extensive data in the complex nearshore region using instruments, a commonly used approach is to estimate LSTR through empirical bulk formulation.

LSTR empirical formulations largely dependent on the field measurements and moreover they remained site specific. Hence, it is important to test these formulations in different coastal regions which are subjected to different wave conditions. In the eastern Arabian Sea, during June-September, a time generally referred to as the summer monsoon or SW monsoon or monsoon, the general direction of

winds is south-westerly and its strength is significantly larger than that during the rest of the year (Kumar et al., 2012). During November-March, winds over the region have an overall north-easterly direction. October and April-May are times of transition (Shetye et al., 1985). This seasonal cycle of winds leads to a cycle in wave field off the west coast of India, both over the open sea and over coastal areas (Kumar and Anand, 2004; Semedo et al., 2011). During the monsoon period the maximum significant wave height along the west coast of India is 6 m and during the non-monsoon period it is less than 1.5 m (Kumar et al., 2003; 2006). Hence, a location off the central west coast of India was selected for the study since the wave conditions of the region vary with the seasons.

Along the west coast of India, quantitative estimation of LSTR was reported at different localities. Prasannakumar (1985) studied sediment transport in the surf zone along certain beaches in Kerala. Chandramohan et al. (1991) estimated LSTR along the north Karnataka coast based on 1-year visual observation of breaking parameters and the longshore currents. In order to examine the various physical processes affecting the different coastal environment of Kerala, an investigation of LSTR was completed by Sajeev (1997). Veerayya and Pankajakshan (1988) have reported longshore sediment transport pattern along the Mangalore coast. Hanamgond (1993) investigated the sediment movement on Aligadde beach, Uttara Kannada and stated that the beach morphology undergoes cyclic seasonal changes in response to the changing wind and wave climate. Other studies on selected coastal segments along the west coast of India for the estimation of annual LSTR include Chandramohan et al. (1994), Jayappa (1996) and Kurian et al. (2009). These studies revealed that the LSTR is variable, bi-directional and season dependent.

Variation in geomorphologic condition can cause large uncertainties in the estimated LSTR and hence field measurements are very important to assess the wave characteristics. Only a few field studies have reported the measurement of LSTR along the central west coast of India. Kumar et al. (2003) studied the LSTR based on measurements along the surf zone of a 4 km-long beach in the central west coast of India over a 4-month period.

LSTR estimates in the above-mentioned studies were largely based on predictive empirical formulations calibrated from field measurements or laboratory physical models (Bayram, 2001; Bayram et al., 2007). Most of the studies along Indian coastline were based on ship reported wave data (Chandramohan et al., 1991) or visually observed wave and littoral environmental observations (Chandramohan and Nayak, 1991; Sajeev, 1997), and numerical modeling to quantify LSTR has not been attempted in many studies.

Most of the LSTR estimates were based on single formulae, and one year-long measured nearshore wave data were not used in these studies for the estimation of LSTR.

Neither long-term nor short-term information on nearshore waves and LSTR were available for the study area in question. Hence, a study was carried out to identify the nearshore wave characteristics and quantify the LSTR from well-known formulation with nearshore wave parameters obtained from the numerical model Delft3D-wave module (Delft Hydraulics, 2011). Measured directional wave data at 3 h intervals for a period of one year were used as input to the numerical model.

The research questions addressed in the study were i) what is the variation in the LSTR estimate using four well known LST formulae, ii) how sensitive are the LSTR estimates to wave height, peak wave period and breaker angle during monsoon and non-monsoon periods, iii) what is the diurnal change in LSTR, and iv) what is the influence of data intervals on the LSTR estimate?

2. Study area

Karnataka's coastline extends over a length of 280 km (Kumar et al., 2006). It is the one of the most indented shorelines with numerous rivers, lagoons, bays, creeks, promontories, cliffs, spits, sand dunes and beaches. Unlike the east coast of India, the coastal stretches of Karnataka have no major delta formation. Also, the coastal zone of Karnataka is one of the better developed regions of the State, with a high degree of economic development and density of population. Areas near the river mouths along the coastline of Karnataka state suffer permanent erosion due to natural shifting and migration of the river mouths (Dattatri, 2007). Erosion becomes severe during monsoon season (June-September) due to high floodwaters in the river and strong wave action (Hegde et al., 2004).

The selected area for study is Kundapura, geographically located at 13˚40'0"N 74˚38'30"E - 13˚36'0"N 74˚42'0"E on the confluence of Kollur, Chakkara and Haladi rivers and Arabian Sea (Fig 1). Sandy beaches, lateritic plain, alluvial plain, tidal flat and Channel Islands are the characteristics of Kundapura.

The coastline at Kundapura is inclined 8º to the west with respect to true north, with the depth contours aligned approximately parallel to the coastline. The depth contours of 10, 20 and 30 m occur at 3, 11 and 20 km from the coast. The mean spring tide range is 1.3 m and the mean neap tide range is 0.61 m (Kumar et al., 2011) indicating that the study area falls in a micro-tidal (tidal range < 2 m) coast.

To understand the offshore wave characteristics of the region, long-term climatology of the study area were examined with ERA-Interim reanalyzed data (Dee et al., 2011) from 1979-2012 at deep water location (water depth ~100 m) (Fig. 2). Waves of this region contain both locally generated wind seas and swells from the southern Indian Ocean. It was observed that about 39% of the waves were approaching from SW and SSW direction and these waves were generally of lower energy (significant wave height, H_s < 1 m) and were observed during the non-monsoon seasons. Waves in the height range of 1-2 m contribute 36% and were evenly distributed in S-W direction. With the onset of the monsoon season, waves from 255-270° become prominent and were similar to the observation of Sajiv et al. (2012) for the central west coast of India. Relatively higher waves (H_s ~ 2-3 m) were approaching from W and WSW and occurred for 16% of time. Higher waves (H_s > 3 m), which were due to the strong winds during the peak monsoon season and storm events, were from the direction between W and WSW and occurred for 4% of the time.

Based on the analysis of beach profiles and textural characteristics of beach sediments, Dora et al. (2011, 2014) observed that during 2008 to 2011, the beaches at Kundapura experienced a slow rate of sediment accretion over an annual cycle. Quantitative study on coastal changes along the study area for the period from 1973 to 2008 was undertaken by Vinayaraj et al. (2011) and reported that the area which covered by the tidal flat, decreased by 0.531 km² during 1973 to 1998 and increased by 0.967 km² during 1998 to 2008. In addition, sand bar environments diminished by an area of 0.227 km² from 1973 to 1998, but during 1998 to 2008 the sand bars show an increasing trend. Few studies have reported LSTR along the central west coast of India (Chandramohan et al., 1991; Chandramohan et al., 1994; Kunte and Wagle, 1993; Kumar et al., 2003) and the LSTR along the study area has not been investigated in the past.

3. Data and methodology

3.1 Measurements

The directional wave data was collected at 3 h intervals using a Datawell directional wave rider buoy at Kundapura (13.61746°N, 74.62234°E) from January to December 2011 at 12 m water depth. Since the waves were measured at 12 m water depth, the measured waves are expected to experience some depth influence and are thus transformed waves. The measured wave height and the wave direction is, therefore, expected to be different than that in the deep water offshore.

LSTR measured by Kumar et al. (2003) using traps deployed on a 4 km-long beach along the Karnataka coast was used for the validation of the LSTR estimates obtained from this study. Two types of traps, one with a circular opening (mesh traps) and other with rectangular (streamer traps) were used in the measurements. Measurements were carried out during February to May 1990 and the breaking parameters were estimated from the wave rider buoy deployed at 16 m water depth. Here, a 4-month dataset is used for validation of the LSTR estimate. During the measurement period, the breaking wave heights were 0.5-1.2 m and the wave periods were 3-9 s. The longshore current velocities were also measured at the trap location. The details of the data collection and analysis are presented in Kumar et al. (2003).

3.2 Wave transformation model description

The wave breaker location changes with change in water level due to the tides and changes with seasons due to change in nearshore profile. Hence, measurement of the wave breaker parameters is difficult and carrying out the LST measurements for a one-year period is not possible. In the absence of the breaking wave characteristics required to assess the quantity of LSTR, numerical modeling techniques are widely used to transform the offshore wave characteristics to the selected location in the breaker zone. The Delft3D-wave module (Delft Hydraulics, 2011) developed by WL|Delft Hydraulics was used to model the nearshore transformation of waves along the study region. Shanas et al. (2014) found that the breaker wave height estimated using Delft3D-wave module was comparable to the measured data with correlation coefficient of 0.73 (p value <0.0005) and root mean square error of 0.07 m. This model is a slightly adapted version of the SWAN model (Booij et al., 1999) which is capable of simulating complicated interactions and transformations experienced by waves propagating through space: refraction due to bottom and current variations, shoaling, blocking and reflections due to opposing currents, transmission/blockage through/by obstacles, effects of wind, white capping, depth-induced wave breaking, bottom friction and non-linear wave-wave interactions. The formulation of Delft3D-wave is based on the spectral wave action balance equation and is fully spectral (in all directions and frequencies). These features range from purely convenient options that allow several different formats for input and output data to options that allow control of fundamental physical processes in the model, like wave generation, dissipation and interaction. The wave computations in Delft3D-wave are unconditionally stable due to the fully implicit schemes that have been implemented. In the Delft3D-

wave module, the governing equation of wave transformation is using action balance spectrum, in geographical space as given below (Ris et al., 1998):

$$\frac{\partial}{\partial t}N + \frac{\partial}{\partial x}C_x N + \frac{\partial}{\partial y}C_y N + \frac{\partial}{\partial \sigma}C_\sigma N + \frac{\partial}{\partial \theta}C_\theta N = \frac{S}{\sigma} \quad (1)$$

where N is the action density spectrum, which is equal to energy density spectrum divided by the relative frequency. In this equation, σ and θ are wave relative frequency and wave direction, respectively. The first term on the left-hand side of this equation represents the local rate of change of action density in time, and the second and third term represent propagation of action in geographical space (with propagation velocities C_x and C_y in x and y space, respectively). The fourth term represents shifting of the relative frequency due to variations in depths and currents (with propagation velocity C_σ in σ-space). The fifth term represents depth-induced and current-induced refraction (with propagation velocity C_θ in θ-space). The right-hand side term of the wave action balance equation is the source term of energy density representing wave generation, energy dissipation and non-linear wave-wave interaction. The term S represents:

$$S = S_{in} + S_{ds} + S_{nl} \quad (2)$$

Waves obtain energy input from wind (S_{in}). The three processes for energy dissipation (S_{ds}) in SWAN are white-capping, bottom friction and depth-induced wave breaking where bottom friction dominates in shallow water whereas white-capping is the main source of energy dissipation in deep water. Energy is transformed between waves by non-linear interactions (S_{nl}). In shallow water, triad wave-wave interactions play a major role, whereas quadruplet wave-wave interactions are important in deep water.

3.2 Input parameters to the wave transformation model

The significant wave height (H_s), peak wave period (T_p) and mean wave direction (θ_p) measured at 12 m water depth was used as the input wave parameters to the model. In this case, one year of data are used to assess the seasonal and annual variations in wave climate. The bathymetry of the study area was obtained by merging the nearshore measured bathymetry data with a digitised naval hydrographic chart No.216 (NHO, 2004). Since there is no restriction for the model on the grid spacing, the selected domain was divided into a rectangular 200 x 200 grid points with a grid spacing of 40 m along both x and y direction. The grid generation was done with 'rgfgrid' of the Delft3D-wave module. The offshore boundary was taken at 12 m water depth since the measured wave data were at this depth. The model

has three types of boundary; i) open boundary in the west where the waves with given height, direction and period propagate into the model area, ii) lateral boundaries at the north and south, and iii) closed boundary in the east (land). No wave can enter the model domain through the eastern boundary and the outgoing waves are fully absorbed in this boundary.

Input at the boundary was taken as a fully spectral approach in the model. The spectral resolution consists of 25 intervals from 0.05-1 Hz. Other input variables for the Delft3D-wave module, such as alpha and gamma for the depth induced breaking (Battjes and Janssen, 1978), were 1 and 0.73 (Battjes and Stive, 1985) and the bottom friction coefficient value was 0.067 (Hasselmann et al., 1973). Table 1 provides a summary of the attributes and input parameters used in the wave transformation model. Model simulation was done for a period of one year from January to December 2011 and the breaking wave characteristics were extracted by applying the breaking criteria (H_s/hb=0.78; CERC, 1984), where hb is the breaking depth. The extracted breaking parameters were used in the formulae below to estimate the longshore current and LSTR.

3.3. Longshore current

Different formulations for longshore current can produce different predictive capabilities for the study area due to use of different input parameters (breaker height, breaker period and beach slope). A longshore current estimate based on Longuet-Higgins depends on breaker height whereas that based on Galvin depends on the wave period. Brocchini (1997) found that the measured longshore current compares well with that estimated based on Longuet-Higgin's with about 15% discrepancy in magnitude. Kumar et al. (2001) found that the longshore current estimated by Galvin was 22% greater than that measured, and that based on Longuet-Higgins was 25% more than the measured current. Since Galvin and Longuet-Higgins formulations are the most commonly used (CERC, 1984) and widely accepted longshore current formulations they were selected for the present study.

i) Longuet-Higgins (1970)

All present-day longshore current models are based on concepts of radiation stress, first introduced by Longuet-Higgins and Stewart (1964). Longuet-Higgins (1970) and others applied these time-averaging principles to the depth-integrated momentum balance equation to obtain the longshore current profile:

$$V = 20.7 m_b (gH_b)^{1/2} \sin(2\alpha_b) \quad (3)$$

ii) Galvin (Galvin and Eagleson, 1965)

Galvin (1965), based his model on the continuity of water mass, arriving at the following equation:

$$V = Kgm_b T(\sin 2\alpha_b) \quad (4)$$

where V = longshore current velocity (m/s), g =acceleration due to gravity (m/s^2), m_b = slope of the bottom in the surf zone, T = wave period (s), H_b = breaking wave height (m), α_b = angle between the breaking wave crest and the local shoreline (deg), K = dimensionless coefficient solely depending on the geometry of the breaking wave (value taken as 1).

3.4. Longshore sediment transport

Since there was no recommended formula for assessing LSTR in the study area, we have chosen 4 different formulations for estimating LSTR which are the most commonly used bulk formulations all around the globe (Bodge and Kraus, 1991; Wang et al., 1998; Kumar et al., 2001; Haas and Hanes, 2004; Khalifa et al., 2009; Mohanty et al., 2012). Using different formulation can yield different estimates of LSTR due to the different parameters in the formulations. The formulation which best matches the field data can be considered as offering reliable estimates of LSTR for the study area. Each of the four different LSTR formulations selected utilizes different input parameters: wave height, wave period, wave direction, grain size, sand porosity, beach slope, sand and water density, wave breaker index, current velocity and empirical coefficients. These models differ in terms of complexity, processes considered, and the data required for model calibration and model use. Since all the parameters influencing LSTR are not included in a single formula, we have tested the most commonly used LST formulae listed below. The Komar (1998), CERC (1984) and Walton and Bruno (1989) formulations are based on the energy flux method. Whereas Kamphuis formula (Kamphuis, 2002) is based on dimensional analysis, derived from extensive laboratory and field studies which include the effect of grain size, beach slope and wave period.

3.4.1. CERC formula (1984)

LSTR was calculated from the empirical equation relating LSTR to the longshore energy flux in the breaker zone. One of the commonly used methods for calculating LSTR is the Coastal Engineering Research Centre (CERC) formula (CERC, 1984). As per the CERC formula, the LSTR is given by:

$$Q = \frac{KA\rho\, g\, H_b{}^2 T \sin(2\alpha_b)}{64\pi} \quad (5)$$

where Q = LSTR (m^3/yr), K = dimensionless empirical proportionality constant (taken as 0.39), $A = \frac{1}{(\rho_s - \rho)g(1-p)}$, ρ_s= sediment density (2650 kg/m^3), ρ = density of water (1030 kg/m^3), g = acceleration due to gravity (9.81 m/s^2) and p = Porosity factor (0.4).

The advantage of the CERC formula is that, due to its simplicity, it enables one to integrate contributions of waves arriving from various directions and to obtain an analytical expression for evaluation of LSTR, but it does not take into account the sediment size and the longshore current.

3.4.2. Kamphuis (2002)

Kamphuis (1991) developed an empirical formula which includes the beach slope, wave period and sediment grain size based on laboratory experiments and existing field data. With additional laboratory data and further analysis, the formula of Kamphuis (2002) was found applicable to both field and experimental data and is given by;

$$Q = \left(\frac{2.27 H_b{}^2 Tp^{1.5} m_b{}^{0.75} d_{50}^{-0.25} \sin(\alpha_b)}{(\rho_s - \rho)g(1-p)} \right) \quad (6)$$

where, Tp = peak wave period (s), d_{50} = sediment median grain size (mm).

Grain size analysis of beach sediments was carried out using an electromagnetic sieve shaker which contains six sieves having mesh sizes such as 2000, 1000, 500, 250, 125, 63 μm along with pan. Median grain size (d_{50}) was extracted by following geometric (modified) Folk and Ward (1957) graphical measures using GRADISTAT (Blott and Pye, 2001).

3.4.3. Walton and Bruno (1989)

Another important formula which is used to calculate LSTR was put forwarded by Walton and Bruno (1989). Using the breaker height and longshore velocity, LSTR was calculated using the formula:

$$Q = \frac{KA\rho\, g\, H_b WVC_f}{0.78\left(5\pi/2\right)\left(\frac{V}{V_0}\right)_{LH}} \quad (7)$$

where, W = Surf zone width (m), C_f = friction coefficient (dimensionless) taken as 0.005 (Kumar et al., 2003), and $(V/V0)_{LH}$ = theoretical dimensionless longshore current velocity with the mixing parameters as 0.4 (Longuet-Higgins, 1970).

3.4.4. Komar (1998)

In this case, LSTR, measured as a volume using the significant wave height proposed by Komar (1998), is given as,

$$Q = 0.46\,\rho g^{3/2} H_b^{5/2} \sin(\alpha_b)\cos(\alpha_b) \quad (8)$$

4. Results and discussion

4.1 Characteristics of measured waves at 12 m water depth

Significant wave height (H_s) was low during the non-monsoon period with monthly average value ranging from 0.5 to 0.7 m (Fig. 3). Wave heights were high in the monsoon season with monthly average H_s ranging from 1.7 to 2.2 m. The average value of H_s during the monsoon was 1.8 m and was similar to the value (1.6 to 1.9) observed during 2009 along the Karnataka coast (Kumar et al., 2012). H_s was more than 1.5 m during 22.8% of the time and the average mean direction of these waves was 263° (Table 2). The average H_s for 2011 was 1 m and that for the deep water region for 34-year period was 1.2 m. The annual average value of H_s for this region was similar to the value of reported for 100 km north of the study region (Sajiv et al. 2012).

Mean wave period (Tz) varied from 2.7 to 10.8 s (Fig. 3). The monthly average Tz during January to April varied between 2.8 and 3.4 s. However, maximum Tz (10.8 s) was observed in the month of October. Average Tz during the monsoon was 6.4 s and was similar to the value (6.5 s) reported for the Karnataka coast in 2009 (Kumar et al., 2012). During the monsoon season there was no significant variation in the wave period, and it mostly persisted between 5 and 7 s, but there was considerable variation in the peak wave period during the non-monsoon period. During the monsoon season, peak wave period was found to be low and mostly persisted between 10 and 12 s. During the one-year period, 86.5% of the waves occurred with peak wave period more than 8 s and these swells had an average mean wave direction of 242° (Table 2). Waves from 220-230° (~SW) dominated during October-May (Fig. 4) and with the onset of monsoon, waves from 250°-270°(WSW-W) became predominant. Mean

wave direction of the highest 10% of the waves was 264°. Mean wave direction was less than 262° during 70% of the time.

Sea breeze has an important influence on alongshore sediment transport in the coastal areas (Pattiaratchi et al., 1997; Masselink and Pattiaratchi, 1998a, 1998b). The studies along the west coast of India has shown that the sea breeze - land breeze system influences the wave parameters during the pre-monsoon period (Glejin et al., 2013). In order to have a clear idea on how the wave parameters in the study area vary throughout the year with sea breeze system, the hourly variation of H_s and Tz in different months was studied (Fig. 5). Strongest sea breezes are generally experienced on hot summer days in tropical and subtropical coastal areas (Masselink and Pattiaratchi, 1998). From the hourly variation of H_s and Tz, it was observed that the wave field was excited by the sea breeze in the afternoon, between 12:00 UTC (17:30 local time) and 17:00 UTC (22:30 local time) (Fig. 5). This result was similar to the observation of Glejin et al. (2013) along the coastal region of Ratnagiri, west coast of India. During the non-monsoon period, wave height reached maximum around this time, with a decrease in mean wave period.

After the onset of the sea breeze, typically late morning or early afternoon, nearshore water levels and incident wave height increases, wave period decreases and wave angle may change depending on the direction of the sea breeze (Sonu et al., 1973). During the study period, the sea breeze effect and diurnal variations in wave height and period was observed throughout the non-monsoon season, whereas the monsoon season lacked diurnal variations in wave parameters. Since land breeze effects were small and in the opposite direction its influence on the swell component is likely to be small. The maximum value of mean wave period was observed during the day hours between 05:00 UTC (10:30 local time) and 09:00 UTC (14:30 local time), due to the presence of long period waves and land breeze system. The role of sea breeze on beach processes and morphology is often masked by the presence of high wave energy levels (Inman and Filloux, 1960). During the monsoon season (June -September), the sea breeze and land breeze effect was masked by the presence of high energy waves due to the strong monsoon winds along the west coast of India.

4.2 Nearshore wave characteristics

Based on the model simulation during January to December 2011, breaking wave characteristics were extracted. Wave transformations for both monsoon and non-monsoon seasons are presented in Fig. 6. During the non-monsoon period, the reduction in wave height across the shore was linear and during the

monsoon period it was non-linear. Maximum H_s measured at the 12-m water depth was up to 3.5 m whereas the breaker height estimated was less than 2.5 m.

Breaker height (H_b) showed seasonal variation (Fig. 7a) similar to the H_s at 12 m water depth. It was found that most of the time during the year, nearshore wave height was less than 1.2 m especially in the non-monsoon period. The most frequently occurring breakers, as seen from the frequency distribution, were those in the height range of 0.6-1.1 m, constituting 55% of the occurrences. More than 70% of the cases fall within the range 0.5 to 1.5 m. H_b was at a maximum during the monsoon season and gradually decreased in other seasons with a secondary peak of comparatively lower magnitude during the post-monsoon season. Average breaker height showed a progressive increase from pre-monsoon to monsoon season. Wave breaker angle was calculated as the difference between the peak wave direction and the direction normal to the depth contour. The breaker angle persisted between -15 and 15° for most of the time during the year (Fig. 7b). Considerable variation in direction of the breaker angle caused variation in the longshore current direction. During the monsoon season, breaker angle mostly persisted between 5 and -10°. During the post-monsoon season, the breaker angle increased and mostly persisted between 8 and 15°, which caused the reversal of longshore current.

4.3 Longshore currents

The coastline along the study area is oriented 8º to the west from the true north. Longshore current direction towards 172° is taken as the flow towards south and that towards 352° is considered north in the study. Estimated longshore currents show significant variations in their direction and magnitude (Fig. 7c, 7d). During January-March, the longshore current direction was transitional and inconsistent, predominantly in northerly direction. During the onset of the monsoon, reversal of longshore current direction was seen and was towards south. The possible cause for the directional shift was due to the changes in wave direction (250°-270°) at the time of onset of the monsoon, with mean wave direction of the highest 10% of the waves as 264°. Since the coastal orientation was 8º to the west from true north, wave direction greater than 262° generated southerly longshore currents. Intense breakers north of the shore-normal direction during the peak monsoon season resulted in strong southerly currents. Again, a reversal of longshore current direction can be seen during the post-monsoon season, with relatively high magnitude towards north. The current speed estimated based on Longuet-Higgins (eq. 3) and that based on Galvin (eq. 4) varied from -0.3 to 0.4 m/s. Both formulae show almost similar variation, with a correlation coefficient of 0.96 (p value <0.001) and hence Longuet-Higgins formula was used in the

Walton and Bruno formula for estimating the LSTR. Chandramohan et al. (1991) studied the daily variation of longshore current velocity along the west coast of India and reported that at Maravande (10 km north of Kundapura), the average longshore current velocity persisted at about 0.3 m/s in June and 0.1-0.15 m/s during the rest of the year. Kumar et al. (2003) reported that the longshore current along the central west coast of India varied from 0.1-0.6 m/s, with an average speed of 0.3 m/s.

4.4 Longshore sediment transport rate

The net LSTR estimated for each month indicate that the direction of LST was from south to north throughout the year (Fig. 8) except during the peak monsoon period (June and July). During the non-monsoon season the wave activity was low (monthly breaker height ranges from 0.5 to 1 m) and with the onset of monsoon, the breaker parameters varied dramatically, which had a direct influence on the transport rate. The wave direction observed during the monsoon season was from WSW-W. The directional shift in the longshore current (shifting from northerly to southerly) and relatively high wave action (average monthly wave height ranges from 1.4 to 1.9 m) prevailing in the monsoon season caused a large amount of sediment transport in a southerly direction. During the post-monsoon season, shifting of direction occurred again and LST was towards north with relatively high magnitude than that during pre-monsoon. Based on visual littoral environmental observations and using Walton and Bruno formula at Maravanthe (10 km north of Kundapura), Chandramohan et al. (1994) reported the direction of LSTR was always north except in May and August.

Since the average H_s during the monsoon period was 3 times the value during non-monsoon period, the estimated LSTR based on the CERC, Walton and Bruno, Kamphuis and Komar formulae during monsoon period (4 months) was 47, 61, 53 and 43%, respectively, of the total LSTR. The non-monsoon period (8 months) contributes to about 53, 39, 47 and 57% based on the same formulae.

The ratio of the monthly net and gross LSTR for the study area was also calculated. The high ratio (~ ±1) of the net and gross LSTR indicates that net LSTR direction is dominating in one direction, predominantly in a northerly direction if the net to gross ratio is close to +1 and a southerly direction if it is close to -1, whereas a low value (~ - 0.5 to +0.5) indicates that northerly as well as southerly transport exist in the area. During the study period, the high net to gross ratio was observed for most of the time (0.75 to 1 during non-monsoon months), which indicates the predominance of northerly LST in the study area. The ratio was found to be low during the monsoon season. During first half of monsoon (June and July), the ratio observed was -0.64 and -0.51 which indicates the bidirectional transport with a

slightly greater southerly transport. In August and September, the ratios observed were 0.64 and 0.69 which also indicates bidirectional transport with a greater northerly transport.

4.4.1 Comparison of estimated LSTR based on different formulae with field data

Inter-comparison between the LSTR estimates based on different formulae (Fig. 9) indicate that the CERC formula overestimates the value by about 1.5, 2.5 and 1.25 times that of Walton and Bruno, Kamphuis and Komar formulae. Reliability of the CERC formula for estimation of LSTR has been discussed over many years (Eversole and Fletcher, 2003; Bayram et al., 2007). One of concerns is the value of the constant K. While K is thought to be affected by the grain size, Komar (1988) could not find a clear relationship because of large scatter of field data. Del Valle (1993) supported the grain-size dependency of K with the field data from a coarse sand coast with a grain size up to 1.5 mm. Schoonees and Theron (1994) calculated the value of K for many field data by grouping them with grain size. For the group with a grain size smaller than 1 mm, the mean value of K is 0.41, while for the group with grain size larger than 1 mm, the mean value is 0.01, although the effect of grain size could not be revealed within the two groups. Van Wellen et al. (2000) used the value of K as 0.07 to fit the data on shingle beaches in their assessment of various longshore transport formulas. In the present study, gross LST of around one million (8.8×10^5) cubic meters of sediment per year from the CERC estimate was found to be unusual and can lead to large coastline variations which were not observed along the study area. Wang et al. (1998) recommended using the CERC formula in storm conditions where the wave heights exceed 4 m. However, in Kundapura coastal region based on the measured wave data, the average H_s was 1 m with maximum value of 3.4 m.

Estimation based on the Komar formulae (gross LSTR = 7×10^5 m^3/yr) was also close to the CERC estimate since the parameters in both the formulae were the same and need to be calibrated for the study area. The Walton and Bruno formulae, which includes the longshore current velocity and surf zone width, estimated annual gross LSTR of 6×10^5 m^3/yr. Annual gross LSTR estimated with the Kamphuis formulae gave a value of 3.1×10^5 m^3/yr. Although the predictive magnitude varies widely, all four formulae agree on the seasonal gross and annual net LST direction. Based on daily littoral environmental observations and use of the Walton and Bruno formula, Chandramohan et al. (1994) reported the annual LSTR at Maravanthe (10 km north of Kundapura) as 0.3×10^5 m^3/yr and at Malpe (30 km south of Kundapura) as 1.07×10^5 m^3/yr. The low values reported may be due to the error in the visual observation of the breaker parameters and the observation of a single day's data.

In order to establish the accuracy of the estimation of LSTR using different formulations, we have compared the estimated LSTR with the measured LSTR. The wave condition at the time of measurement and present study period were compared to illustrate that the wave conditions were similar. The average wave conditions (significant wave height) at the measurement site for pre-monsoon, monsoon and post-monsoon season were 0.8, 1.7 and 0.5 m (Kumar et al. 2012). Similar wave conditions, with average wave height of 0.7, 1.8 and 0.5, were observed during the study period. During their field experiment, Kumar et al. (2003) measured both the lateral and vertical distributions of the sediment transport rate with traps deployed in a line spanning the surf zone during February to May along the central west coast of India. They reported an average gross LSTR of 726 m^3/day. In the present study, the average gross transport rate estimated for the same period was 1265, 1092, 694, 1097 m^3/day based on the CERC, Walton and Bruno, Kamphuis and Komar formulae, respectively. The comparison of daily average LSTR with measured daily average LSTR for different formulations and similar analysis on a monthly basis was also completed (Fig. 10). The comparison showed very good correlation for the estimated LSTR using the Kamphuis formula, with a small root mean square error in monthly average LSTR of 21 m^3/day and high correlation coefficient of 0.98 (p value 0.016). Other formulae showed large scatter with considerable over-prediction in monthly averaged LSTR (Table 4). Since, the Kamphuis formula is in close agreement with the measured data, the same is considered more suitable for the study area. This study shows that the Kamphuis formula can be used for locations with annual average H_s of 1 m. Wang et al. (2002) observed that the Kamphuis formula is preferable in low-wave energy conditions since it gives more consistent predictions for both spilling and plunging breaking wave conditions due to inclusion of wave period in the expression, which has significant influence on breaker type.

4.4.2 Correction applied to LSTR formulae

Comparison of estimated LSTR value with the measured field data shows that with the exception of the Kamphuis formula, the values estimated based on other formulae were more high. Suitable correction factors were determined to make the estimations more realistic and acceptable with the available target (observed) values (Fig. 11). Correction factors (Cor_{CERC}=0.38, Cor_{Walton}=0.58, and Cor_{Komar}=0.49) were applied, which resulted in improved LSTR estimates in closer agreement with the target value for the study area (Table 5). Such studies were also reported for two bulk-type formula (CERC and Van Rijn) for the Egyptian northern coast, where the correction factor for the CERC formula was found to be 0.2

(Khalifa et al., 2009). No correction factor was needed for the Kamphuis formula since its evaluations were close to the measured values.

4.4.3 Influence of breaker parameters on LSTR

Along the study area, during the monsoon period, the beaches were strongly influenced by breaking waves, resulting in erosion processes (Dora et al., 2014) and onshore-offshore transport of sand. Smith et al. (2009) observed that LSTR was mainly influenced by the breaker parameters. Direction of LST largely depends on the direction of incoming waves with respect to shoreline which, in turn, determines the direction of the longshore current. Since the Kamphuis formula shows close agreement with the field data, LSTR based on this formula was used to study the influence of breaker parameters on LSTR. The analysis was done for both, monsoon (June-September) and non-monsoon periods (Fig. 12). It was found that during the non-monsoon period, most of the waves were low energy long period swells. It was clearly observed that during the non-monsoon period the variation of LSTR largely depends on the breaker height, and the effect of breaker angle on LSTR was small compared to breaker height. During the monsoon season, the variation of LSTR depends more strongly on breaker angle than breaker height (Fig. 12). During the monsoon season, wave energy was high during most of the time and the direction of wave approach was close to shore-normal. Thus, a slight change in the wave direction altered the LSTR, indicating that LSTR was more sensitive to the breaker angle during the monsoon season. About 57% of the waves were long period waves with periods more than 12 s during the non-monsoon period and resulted in high LSTR. During the monsoon season, most of the waves (70%) were swells with intermediate peak wave periods (10-12 s). Hence, peak wave periods in the range 10-12 s drive a large proportion of LSTR during the monsoon season, whereas during the non-monsoon period, peak wave period of more than 12 s contributes significantly to LSTR.

The LSTR shows significant scattering with breaker angle during the non-monsoon period and with breaker height during monsoon period, which underlines the sensitivity of breaker angle and breaker height on the estimation of LSTR in different seasons. Estimated LSTR using the Kamphuis formula with breaker height shows more scatter (correlation coefficient, $r=0.76$ and p value <0.001) than that based on CERC ($r=0.78$, p value <0.001), Walton and Bruno ($r=0.8$, p value <0.001) and Komar ($r=0.81$, p value <0.001) which shows the influence of other parameters (grain size, peak wave period and beach slope) on LSTR. Monthly variation of median grain size (Fig. 13) also indicates that the grain

size was greater during the monsoon season compared to the non-monsoon season, which in turn slightly decreases the transport rate.

This study shows that 82% of the LSTR was due to the waves approaching from the sector between 225 and 270°, and 83% of this transport was towards the north and the balance of 17% was towards south. For the study area, waves were from the sector between 225 and 270° during 72% of the time (Fig. 4). Waves approaching from the sector between 270 and 315° contribute only 9.5% of the gross LSTR and those from the sector between 180 and 225° contribute 8.5% of the gross LSTR. The estimated annual gross LSTR based on the Kamphuis formula, considering the breaker parameters at 2.2 m water depth, 3% higher than that estimated at the actual breaker point.

4.4.4 Influence of data interval on LSTR estimation

In order to investigate the influence of data interval on LSTR, the 3 h variation of LSTR with different wave parameters was analyzed for different months in a year. Fig. 14 illustrates the 3 h variation of LSTR with breaker angle, breaker height and peak wave period. During the monsoon months, the breaker angle and LSTR shows an almost similar pattern, whereas during the non-monsoon season considerable variation was observed. Relatively small changes in breaker angle during the monsoon season changes the LSTR (Fig. 14). During the February to May, generally the LSTR was high during the day hours and was in accordance with the sea breeze system. The onset of sea breeze increases the wave height, as a consequences LSTR increase dramatically (Fig. 14). During January, variation in LSTR was similar to the variation of Tp, H_b and breaker angle. During February to April and October to December, the variation of LSTR was diurnal and opposite to the variation of Tp (Fig. 14). Southerly transport was observed only in June and July.

Since the hourly variation of wave properties was influenced by sea/land breeze system, we have examined the variation of LSTR based on a single dataset collected at a different time in a day with that based on all data (Fig. 15). The annual net and gross LSTR was less than the estimate based on all data for estimates based on data collected up to 9 h and was more for the estimate based on remaining period. Large variations of up to ~17% in annual net and ~5% in annual gross estimates were observed in the LSTR estimate based on data at different time compared to the estimate based on all data.

Continuous site-specific data collection in the coastal area is costly and difficult due to interferences from fishing vessels. Hence, in the past the annual LSTR were estimated based on the data collected at

daily to monthly intervals. We have examined the variation in monthly net and gross LSTR using the Kamphuis formula by considering different data intervals ranging from 3 to 24 h. The difference in LSTR for data at 3 and 6 h intervals were maximum during the month of July and August (9.9% and 10.8%), whereas the difference was negligible during November. During November, most of the time, waves were approaching from a SW direction and throughout the month northerly transport was observed. The breaker height was also not varying much in November; about 80% of the time breaker height was in the range 0.5-0.8 m and hence, the difference in LSTR based on different data interval was less. However, the LSTR estimates can result in a large error if the wave characteristics change during a short period of time. During the monsoon period, especially during the months July and August, the difference in LSTR based on different data intervals was high due to the large variation in the wave characteristics during a short period of time. On the other hand, data at 12 h resulted in a difference in LSTR up to 13% compared to 3 h. The difference in LSTR at 3 and 24 h intervals was up to 24%. The study shows that the error in LSTR estimate based on different data intervals will be a minimum for areas which are subject to small temporal changes in wave characteristics.

Similarly, the daily average breaker parameters were calculated from the 3 h data for the study period and LSTR was estimated using these daily averaged breaker parameters. The results obtained from the daily average parameter and that estimated using 3 h data were compared. The results show that there was about 16% reduction in annual net LSTR and 12% in the annual gross LSTR if the daily average parameters were used in the calculation.

5. Conclusions

The variation in the LSTR estimate using the four bulk formulae, the CERC, Walton and Bruno, Kamphuis and Komar formulae were examined based on the nearshore wave data measured for one-year period at 12 m water depth and the wave transformation model DElft3d-wave module. The waves from 220°-230° (~SW) dominates during October-May, and with the onset of monsoon waves from 250°-270°(WSW-W) become predominant. The average breaker wave height during pre- and post-monsoon seasons were found to be low (0.7 m) and high (1.7 m) during monsoon season. The study shows that for locations with annual average H_s of 1 m, the Kamphuis formula can be used to estimate LSTR. Estimated transport rates based on other formulae were quite high and require correction. Suitable correction factors (Cor_{CERC}=0.38 ,Cor_{Walton}=0.58, and Cor_{Komar}=0.49) are determined for making the

LSTR estimates more realistic and acceptable for the study area. Since the average H_s during the monsoon period was 3 times the value during pre- and post-monsoon periods, the LSTR during the monsoon period (4 months) was 53% of the total LSTR and that during the non-monsoon period (8 months) was 47%. LST direction depends on the direction of incoming waves and on the angle between the wave crest and the shoreline, which also determines the direction of longshore current. It is found that the influence of breaker height is greater during the non-monsoon periods whereas during the monsoon period, breaker angle shows greater influence on LSTR. The study emphasizes the need to have closer data interval for estimating LSTR at a particular region. For better and more accurate estimates of LSTR, the data interval should be 3 h or less.

Acknowledgment

The study was part of the project on shoreline management plans for Karnataka coast. We thank the Integrated Coastal and Marine Area Management Project Directorate (ICMAM PD), Ministry of Earth Sciences, New Delhi for funding the project. Director, CSIR-National Institute of Oceanography, Goa and Director, ICMAM PD, Chennai provided encouragement to carry out the study. We thank the two anonymous reviewers for their constructive comments and suggestions which substantially improved the paper. The first author acknowledges Department of Science & Technology, New Delhi for awarding the INSPIRE fellowship. This is NIO contribution xxxx.

References

Battjes, J.A., Janssen, J.P.F.M., 1978. Energy loss and set-up due to breaking of random waves. Proceedings 16 International Conference in Coastal Engineering, ASCE, 569-587.

Battjes, J.A., Stive, M.J.F., 1985. Calibration and verification of a dissipation model for random breaking waves. J. Geophys. Res. 90 (C5), 9159-9167.

Bayram, A., Larson, M., Hanson, H., 2007. A new formula for the total longshore sediment transport rate. Coast. Engg. 54, 700-710.

Bayram, A., Larson, M., Miller, H.C., Kraus, N.C., 2001. Cross-shore distribution of longshore sediment transport: comparison between predictive formulas and field measurements. Coast. Engg. 44, 79-99.

Blott, S.J., Pye, K., 2001. GRADISTAT: a grain size distribution and statistics package for the analysis of unconsolidated sediment. Earth Surface Processes and Landforms. 26, 1237-1248.

Bodge, K.R. Kraus, N.C., 1991. Critical examination of longshore transport rate amplitude. In: Proceedings of Coastal Sediments. 139-15

Booij, N., Ris, R.C., Holthuijsen, L.H., 1999. A third generation wave model for coastal regions. Model description and validation. J. Geophys. Res. 104 (C4), 7649-7666.

Brocchini, M., 1997. Eulerian and Lagrangian aspects of the longshore drift in the surf and swash zones. J. Geophys. Res. 102(10), 23155-23168.

CERC, 1984. Shore Protection Manual. Vols I and II. Coastal Engineering Research Center. U.S. Army Corps of Engineers, Washington, DC: U.S. Government Printing Office, Vicksburg.

Chandramohan, P., Nayak, B.U., 1991. Longshore sediment transport along the Indian coast. Indian. J. Mar. Sci. 20,110-114.

Chandramohan, P., Kumar, V.S., Nayak, B.U., Raju, N.S.N., 1994. Surf zone dynamics along the coast between Bhatkal and Ullal, West Coast of India. Indian. J. Mar. Sci. 23, 189–194.

Dattatri, J., 2007. Coastal erosion and protection along Karnataka coast, Centre for Environmental Law, Education, Research and Advocacy (CEERA), The National Law School of India University. http://www. nlsenlaw.org/live/nlsenlaw/crz/articles.

Dee, D.P., Uppala, S.M., Simmons, A.J., Berrisford, P., Poli, P., Kobayashi, S. and Coauthors, 2011. The ERA-Interim reanalysis: configuration and performance of the data assimilation system. Quarterly J. Royal Meteorological Society, 137, 553–597.

Del Valle, R., Medina, R., Losada, M.A., 1993. Dependency of coefficient K on grain size. J. Waterway, Port, Coastal, Ocean. Eng. 119(5), 568-574.

Dora, G.U., Kumar, V.S., Philip, C.S. Johnson, G., 2014. Quantitative estimation of sediment erosion and accretion processes in a micro-tidal coast. Indian J. Mar Sci. (in press).

Dora, G.U., Kumar, V.S., Philip, C.S., Johnson, G., Vinayaraj, P., Gowthaman, R., 2011. Textural characteristics of foreshore sediments along Karnataka shoreline, west coast of India. Int. J. Sediment Res. 26, 364-377.

Eversole, D., Fletcher, C.H., 2003. Longshore sediment transport rates on a reef-fronted beach: field data and empirical models Kaanapali Beach, Hawaii. J. Coast. Res. 19(3), 649– 663.

Folk, R.L., Ward, W.C., 1957. Brazos River bar: a study in the significance of grain size parameters. J. Sedimentary Petrology. 27, 3–26.

Galvin, C.J., Eagleson, P.S., 1965. Experimental study of longshore currents on a plane beach: U. S. Army Corps of Engineers. Coastal Engineering Research Center, TM-10.

Glejin, J., Kumar, V.S., Nair, T.M.B., Sing, J., 2013. Influence of winds on temporally varying short and long period gravity waves in the near shore regions of eastern Arabian Sea. Ocean Sci., 9, 3021–3047.

Güner, H.A. Arı, Yüksel, Y.,. Çevik, E.O., 2013. Longshore Sediment Transport-Field Data and Estimations Using Neural Networks, Numerical Model, and Empirical Models. J. Coast. Res. 29 (2), 311 – 324.

Haas, K., Hanes, D., 2004. Process based modeling of total longshore sediment transport. J. Coast. Res. 20(3), 853-861.

Hanamgond, P.T., 1993. Morphological and sedimentological studies within Kavada Bay and Belekeri Bay beaches, Uttara Kannada district, Karnataka, West coast, India. Unpublished Ph.D. thesis, Karnataka University, Dharward, India, 265 p.

Hasselmann, K., Barnett, T.P., Bouws, E., Carlson, H., Cartwright, D.E., Enke, K., Ewing, J.A., Gienapp, H., Hasselmann, D.E., Kruseman, P., Meerbrug, A., Muller, P., Olbers, D.J. Richter, K. Sell, W., Walden, H., 1973. Measurements of wind- wave growth and swell decay during the Joint North Sea Wave Project (JONSWAP). Deutsche Hydrographische Zeitschrift. A80(12), 95 p.

Hegde, V.S., Gosavi, K.D., Hanamgond, P.T., Huchchannavar, G.K., Shalini, G., Bhat. M.S., 2004.Depositional environment and silting in the Sharavati estuary, central west coast of India. Indian J. Mar. Sci. 33(3), 296–302.

Inman, D.L., Filloux, J., 1960. Beach cycles related to tide and local wind regime. J. Geol. 68, 225–231.

Jayappa, K.S., 1996. Longshore sediment transport along the Mangalore Coast, west coast of India. Indian J. Mar. Sci. 25, 157-159.

Jiang, W. A., Hughes, M., Cowell, P., Gordon. A., Savioli, J.C, Ranasinghe, R., 2010. A hybrid model of swash-zone longshore sediment transport on reflective beaches. In: Proc. 32 Conference on Coastal Engineering, Shanghai, China, 1-12.

Kamphuis, J.W., 1991. Alongshore sediment transport rate. J. Waterway, Port, Coastal and Ocean Eng. ASCE 117 (6), 624–641.

Kamphuis, J.W., 2002. Alongshore transport of sand. In: Proc. 28 Coastal Engineering Conference, ASCE. 2478-2490.

Khalifa, M.A., El Ganainy, M.A., Nasr, R.I., 2009. Wave transformation and longshore sediment transport evaluation for the Egyptian northern coast, via extending modern formulae. J. Coast. Res. 25(3), 755– 767.

Komar, P.D., 1998. Beach Processes and Sedimentation. Prentice Hall Inc. New Jersey, 544–545.

Kumar, V.S., Anand, N.M., 2004. Variations in wave direction estimated using first and second order Fourier coefficients. Ocean Eng. 31, 2105–2119.

Kumar, V.S., Anand, N.M., Chandramohan, P., Naik, G.N., 2003. Longshore sediment transport rate-measurement and estimation, central west coast of India. Coast. Eng. 48, 95–109.

Kumar, V.S., Dora, G.U., Philip, S., Pednekar, P., Singh, J., 2011. Variations in tidal constituents along the near shore waters of Karnataka. west coast of India. J. Coast. Res. 27 (5), 824-829.

Kumar, V.S., Johnson, G., Dora, G.U., Philip, S.C., Singh, J., Pednekar, P., 2012. Variations in near shore waves along Karnataka, west coast of India. J. Earth Syst. Sci. 121, 393-403.

Kumar, V.S., Kumar, K.A., Raju, N.S.N., 2001. Nearshore processes along Tikkavanipalem beach, Visakhapatnam, India, J. Coast. Res. 17(2), 271-279.

Kumar, V.S., Pathak, K.C., Pednekar, P., Raju, N.S.N., Gowthaman, R., 2006. Coastal processes along the Indian coastline. Curr. Sci.91(4), 530–536.

Kunte, P.D., Wagle, B.G., 1993. Remote sensing approach to determine net shore drift direction - A case study along the central east coast of India. J. Coast. Res. 9(3), 663- 672.

Kurian, N.P., Rajith, K., Sheela Nair, L., Shahul Hameed, T.S., Ramana Murty, M.V., Arjun, S., Shamji, V.R., 2009. Wind waves and sediment transport regime off the south-central Kerala coast, India. Nat. Hazards. 49, 325–345.

Longuet-Higgins, M.S., 1970. Longshore current generated by obliquely incident sea waves. J. Geophy. Res. 75 (33), 6778–6789.

Mafi, S., Yeganeh-Bakhtiary, A., Kazeminezhad, M.H., 2013. Prediction formula for longshore sediment transport rate with M5' algorithm In: Proceedings 12th International Coastal Symposium (Plymouth, England), J. Coast. Res, Special Issue No. 65, 2149-2154, ISSN 0749-0208.

Masselink, G., Pattiaratchi, C.B., 1998b. Morphodynamic impact of sea breeze activity on a beach with beach cuspmorphology. J. Coast. Res. 14/2, 393–406

Masselink, G., Pattiaratchi., C.B., 1998a. The effects of sea breeze on beach morphology, surf zone hydrodynamics and sediment resuspension. Mar. Geol. 146,115–135.

Mil-Homens, J.P., Ranasinghe, R.W.M.R.J.B., Van Thiel de Vries, J.S.M., Stive, M.J.F., 2012. Re-assessment and update of bulk longshore sediment transport formulas. ICCE 2012: Proceedings of the 33 International Conference on Coastal Engineering, Santander, Spain, 1-6 July 2012.

Mohanty, P.K., Patra, S.K., Bramha, S., Seth, B., 2012. Impact of Groins on Beach Morphology : A Case Study near Gopalpur Port , East Coast of India. J. Coast. Res. 28 (1), 132–142.

NHO, 2004, India-West coast: Belekeri to Kundapura (Coondapoor), Hydrographic chart no. 216, Published at the National Hydrographic Office, Dehradun; India .

Pattiaratchi, C., Hegge, B.J., Gould, J., Eliot, I.G., 1997. Impact of sea breeze activity on near shore and foreshore processes in Southwestern Australia. Cont. Shelf Res. 17,1539-1560.

Prasannakumar, S., 1985. Studies on sediment transport in the surf zone along certain beaches of Kerala. Unpubl. Ph.D. thesis, Cochin Univ. of Sci. and Tech., Cochin, 110 p.

Ris, R.C., Booij, N., Holthuijsen, L.H., 1998. A third- generation wave model for coastal regions, part II: verification. J. Geophy. Res. 104 (C4), 7649–7666.

Sajeev, R., Chandramohan, P., Josanto, V., Sankaranarayanan, V.N., 1997. Studies on sediment transport along Kerala Coast, Southwest coast of India. Indian. J. Mar. Sci. 26(1), 11-15.

Sajiv, P.C., Kumar, V.S., Johnson, G., Dora, G.U., Vinayaraj, P,. 2012. Interannual and seasonal variations in near shore wave characteristics off Honnavar, west coast of India, Current Science 103 (3), 286-292.

Schoonees, J.S., Theron, A.K., 1994. Accuracy and applicability of the SPM longshore transport formula. Proceedings of the 24 Coastal Engineering Conf. ASCE, 2595-2609.

Semedo, A., Suselj, K., Rutgersson, A., Sterl, A., 2011. A Global View on the Wind Sea and Swell Climate and Variability from ERA-40. J. Climate 24, 1461-1479.

Shanas, P.R., Kumar, V.S., C, Glejin, J., Philip, S., Dora, U.G., 2014. Comparison of formulae for longshore transport of sand along Malpe, west coast of India, Journal of Hydro-environment Research (under revision).

Shetye, S.R., Shenoi, S.S.C., Antony, A.K., Kumar, V.K., 1985. Monthly-mean wind stress along the coast of the north Indian Ocean. J. Earth Syst. Sci. 94, 129-137

Smith, E.R., Wang, P., Ebersole, B.A., Zhang, J., 2009. Dependence of total longshore sediment transport rates on incident wave parameters and breaker type. J. Coast. Res. 25(3), 675–683.

Sonu, C.J., Murray, S.P., Hsu, S.A., Suhayda, J.N., Waddell, E., 1973. Sea-breeze and coastal processes. EOS, Trans. AGU, 54, 820–833.

Van Rijn, L.C., 2002. Approximation formulae for sand transport by currents and waves and implementation in DELFT-MOR. Report Z3054.20, Delft Hydraulics, Delft, The Netherlands.

Van Wellan, E., Chadwick, A.J., Mason, T., 2000. A review and assessment of longshore sediment transport equations for coarse-grained beaches. Coast. Engg. 40, 243-275.

Veerayya, M., Pankajakshan, T., 1988.Variability in wave refraction and resultant near shore current patterns: Exposed versus sheltered beaches along North Karnataka, west coast of India. Indian J. Mar. Sci. 17(2), 102-110.

Vinayaraj, P., Johnson, G., Dora, G.U et al., 2011. Quantitative Estimation of Coastal Changes along Selected Locations of Karnataka, India : A GIS and Remote Sensing Approach. Ocean Eng. 2011:385–393. doi: 10.4236/ijg.2011.24041.

Walton, T.L., Bruno, R.O., 1989. Longshore transport at a detached breakwater, Phase-II. J. Coast. Res. 65(9), 667-668.

Wang, P., Ebersole, B. A., Smith, E. R., 2002. Longshore sand transport – initial results from large-scale sediment transport facility, ERDC/CHL CHETNII-46, U.S. Army Engineer Research and development Center, Vicksburg, MS. http://chl.erdc.usace.army.mil/.

Wang, P., Kraus, N.C., Davis, R.A., 1998.Total longshore sediment transport rate in the surf zone: field measurements and empirical predictions. J. Coast. Res. 14(1), 269–282.

WL Delft Hydraulics. 2011. Delft3D-Wave User Manual. Delft, The Netherlands.

Table 1. Summary of the attributes and some input parameters used in the wave transformation model

Delft3d_SWAN Attributes		**Variable input**	**value**
Basis of model formulation	Action density spectrum	spectral resolution	25 intervals from 0.05-1 Hz
Sector of wave propagation	360°	Time interval	3 h
Steady state /time dependent	Time dependent	Grid dimension	200x200
Wind field / tidal forcing	Not included	Grid spacing	~ 40 m
Current input/wave current interaction	Not included	Directional spread	4 (default)
Wave breaking model	Statistical Battjesand Janssen (1978)	breaking coefficient (γ)	0.73
Bottom friction	Jonswap (Hasselmann, 1973)	C_{bottom}	0.067

Table 2. Statistics of wave parameters. Mean (μ) and standard deviations (σ) are presented for each variable

Sub set description	H_s (m) ($\mu \pm \sigma$)	Tz (s) ($\mu \pm \sigma$)	Tp (s) ($\mu \pm \sigma$)	θp (deg) ($\mu \pm \sigma$)
All waves	1.0 ± 0.7	5.5 ± 1.3	11.6 ± 3.2	249 ± 26
Highest 10% of waves	2.5 ± 0.3	6.8 ± 0.5	11.1 ± 1.8	264 ± 11
Waves with Tp > 8 s	1.1 ± 0.7	5.7 ± 1.3	12.5 ± 2.5	242 ± 18
Waves with Tp ≤ 8 s	0.7 ± 0.2	4.3 ± 0.8	5.9 ± 1.1	294 ± 25
Waves with Hs > 1.5 m	2.1 ± 0.4	6.6 ± 0.6	10.8 ± 1.6	263 ± 11
Waves with Hs ≤ 1.5 m	0.7 ± 0.3	5.2 ± 1.3	11.9 ± 3.6	245 ± 28
Waves during pre-monsoon period (February-May)	0.7 ± 0.2	4.5 ± 0.9	11.8 ± 3.8	249 ± 31
Waves during monsoon period (June-September)	1.8 ± 0.6	6.4 ± 0.7	11.0 ± 2.0	259 ± 13
Waves during post-monsoon period (October-January)	0.6 ± 0.2	5.5 ± 1.5	12.1 ± 3.5	239 ± 27
Waves with θp > 262°	1.5 ± 0.8	5.5 ± 1.3	8.5 ± 2.4	282 ± 18
Waves with θp ≤ 262°	0.8 ± 0.5	5.5 ± 1.4	12.9 ± 2.6	235 ± 13

Table 3. Estimated annual net and gross longshore sediment transport rate

	Estimated LSTR (10^5 m^3/yr)			
Annual	CERC	Walton and Bruno	Kamphuis	Komar
Net	3.60	3.0	1.63	2.55
Gross	8.80	6.0	3.10	7.01

Table 4. Comparison of estimated LSTR with measured field data for different formulations.

Formula used	RMSE (m^3/day)	Mean bias (m^3/day)	SI	CC
CERC	1006.75	-878.25	1.37	0.93
Walton and Bruno	863.89	-845.50	1.17	0.94
Kamphuis	71.73	-21.75	0.10	0.98
Komar	735.60	-623.25	1.00	0.92

Table 5. Estimated annual net and gross longshore sediment transport rate after applying correction factor

	Estimated annual net and gross LSTR after correction (10^5 m^3/yr)			
Annual	CERC	Walton and Bruno	Kamphuis	Komar
Net	1.37	1.78	1.63	1.25
Gross	3.34	3.49	3.10	3.43

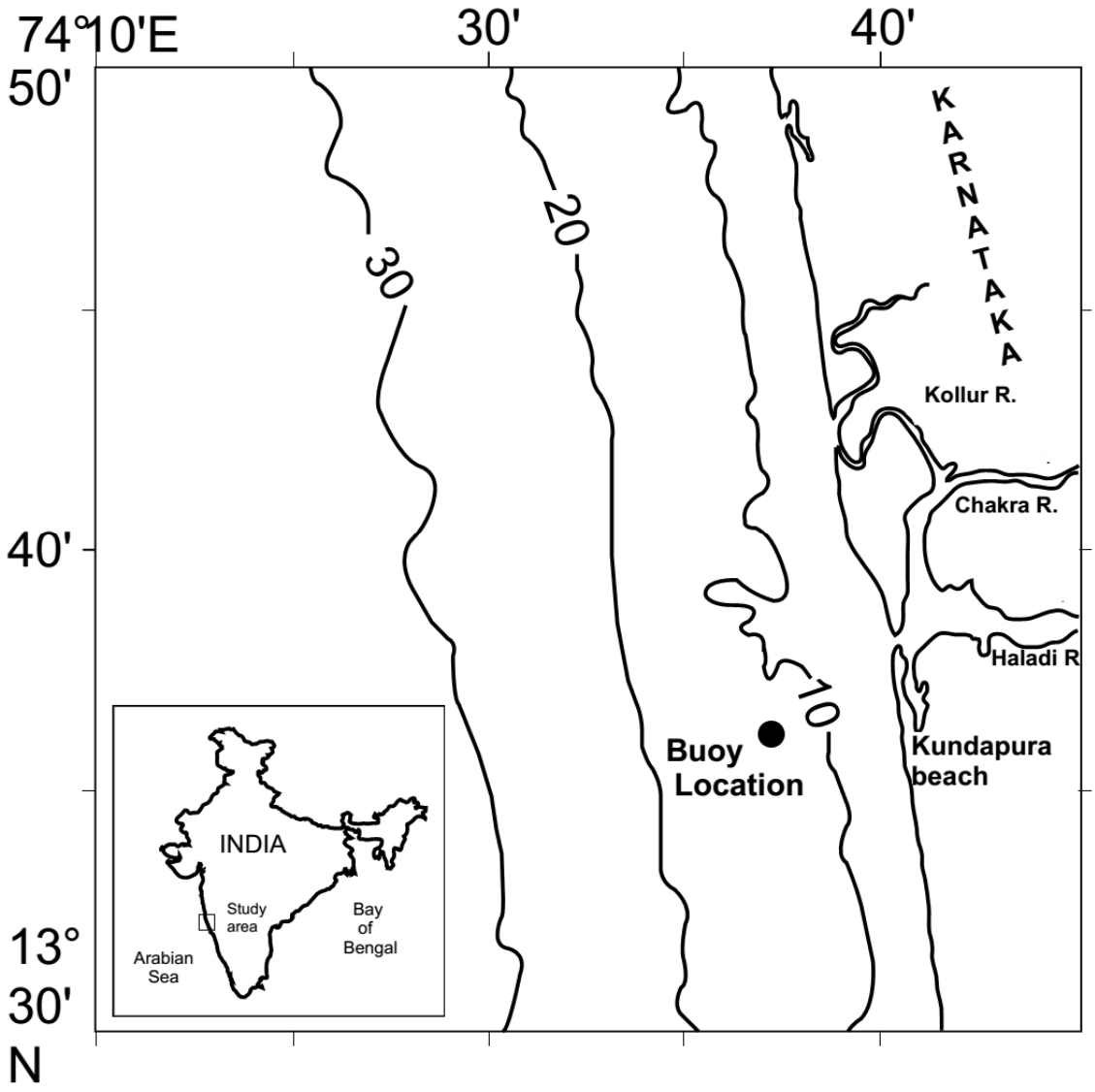

Figure 1. Study area showing the Kundapura beach and the location of wave measurements. The depth contours are in metres.

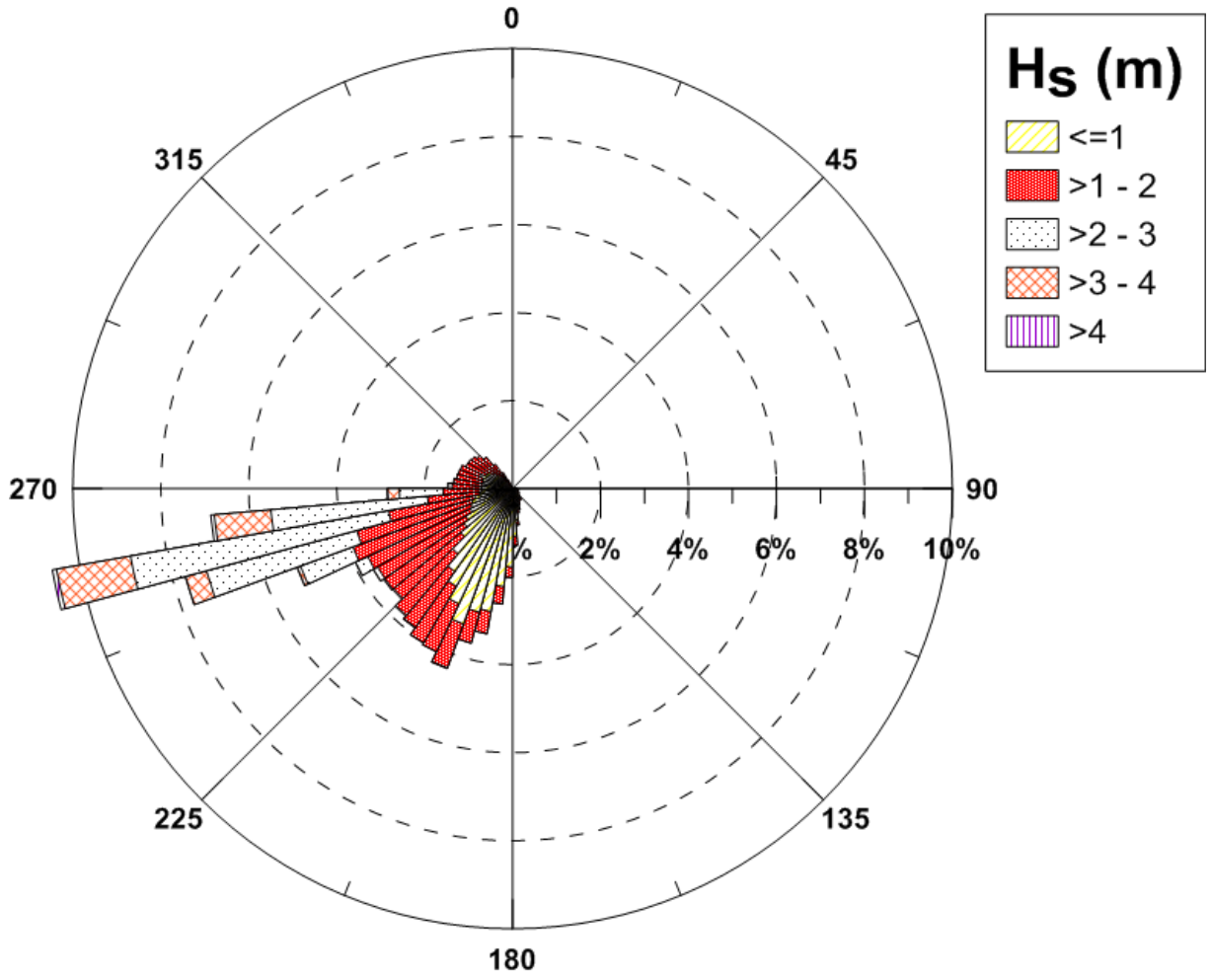

Figure 2. Long term wave statistics of Kundapura at deep water location using ERA-Interim reanlysed data during 1979-2012

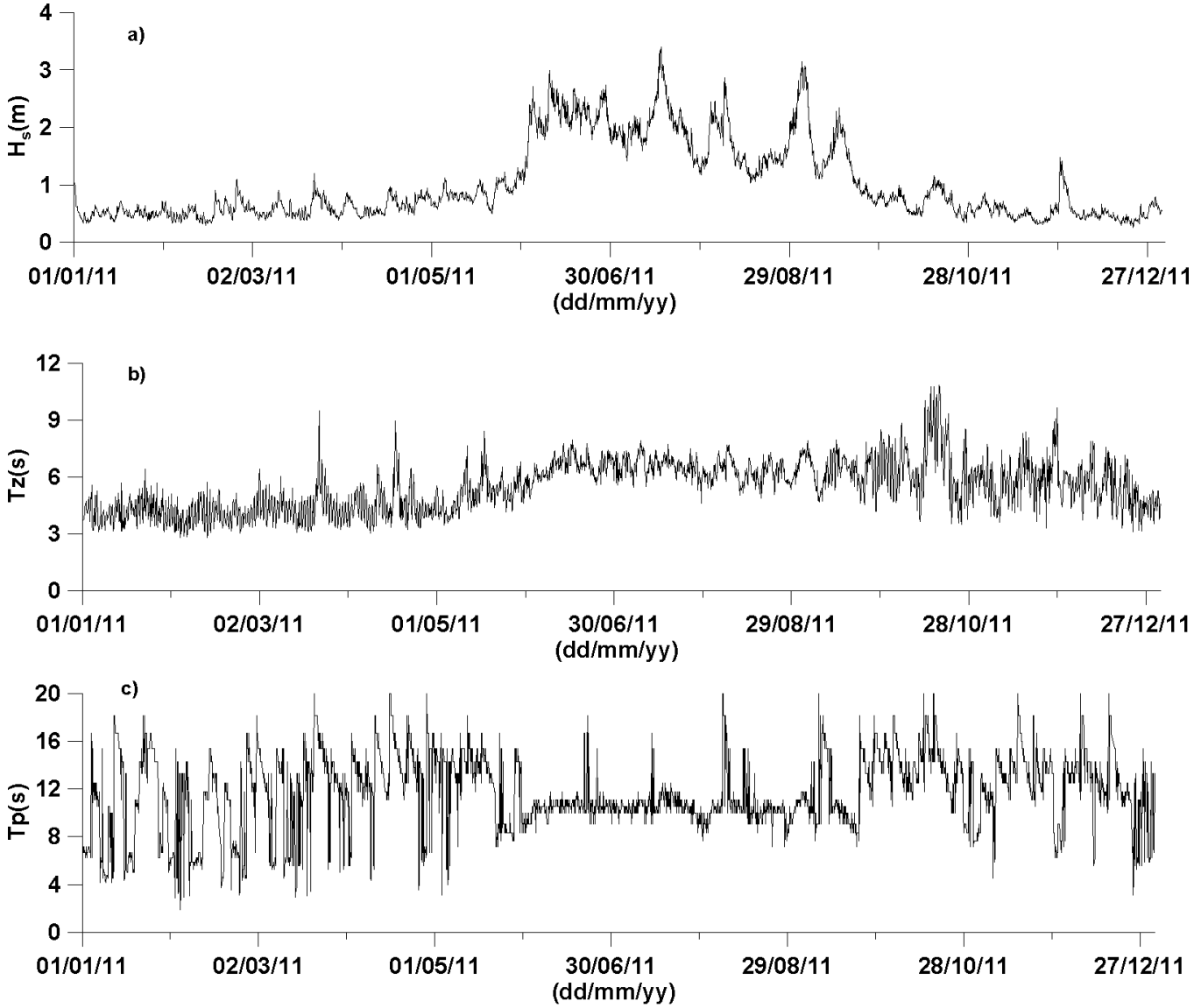

Figure 3. Variation of significant wave height (H_s), mean wave period (Tz) and peak wave period (Tp) measured at 12 m water depth.

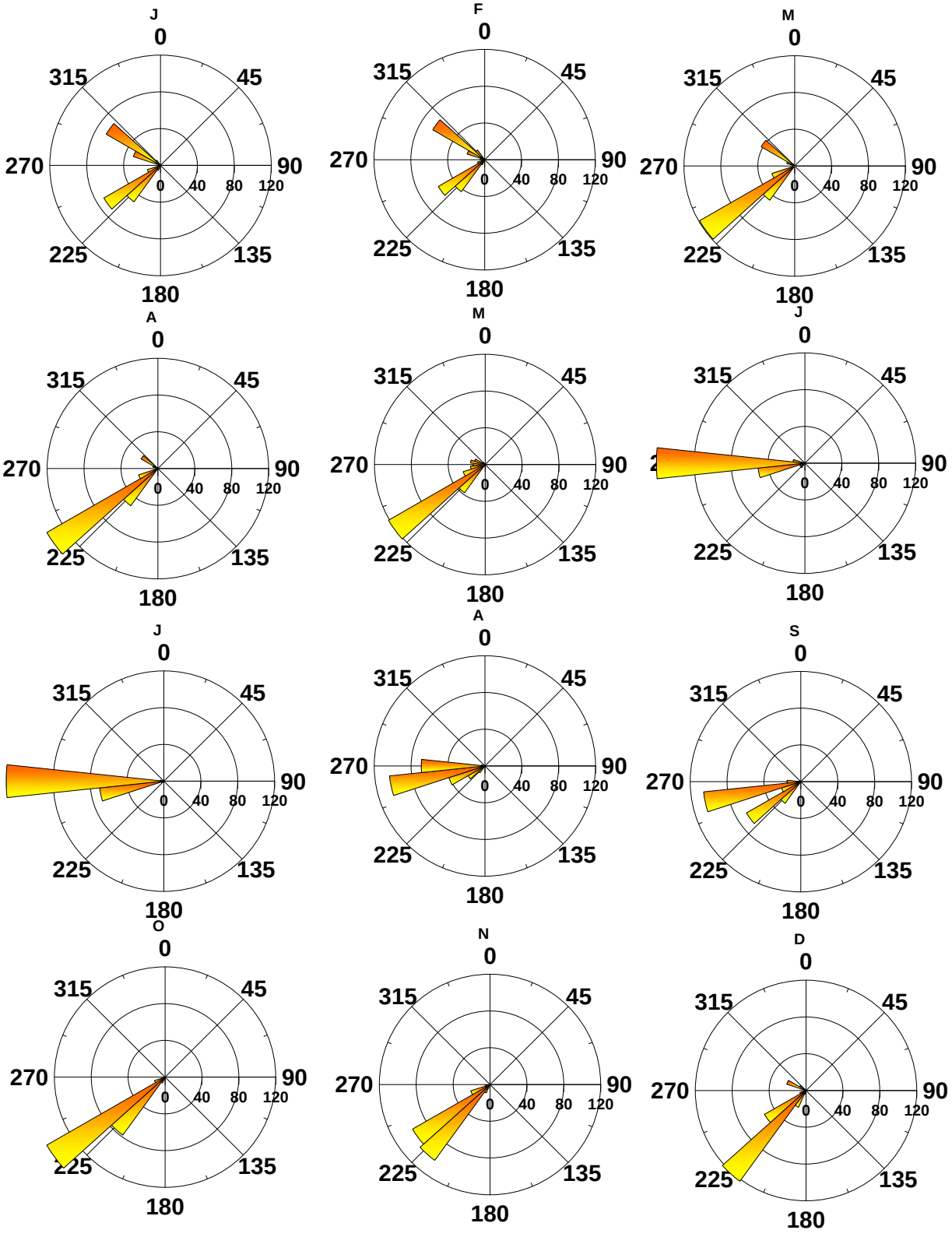

Figure 4. Rose diagram of mean wave direction measured at 12 m water depth in different months

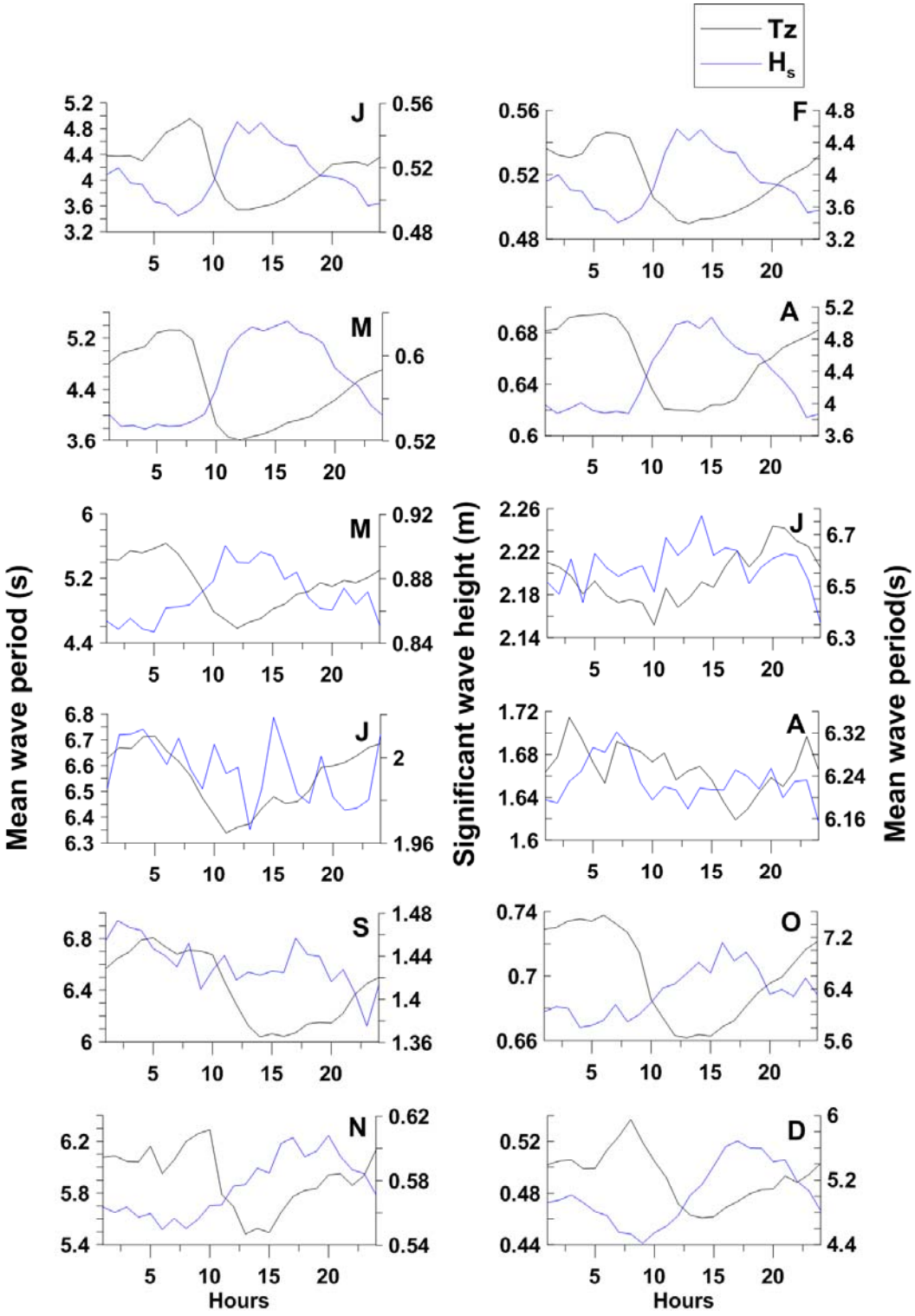

Figure 5. Hourly variation of H_s and Tz during 2011 at 12 m water depth based on measured data

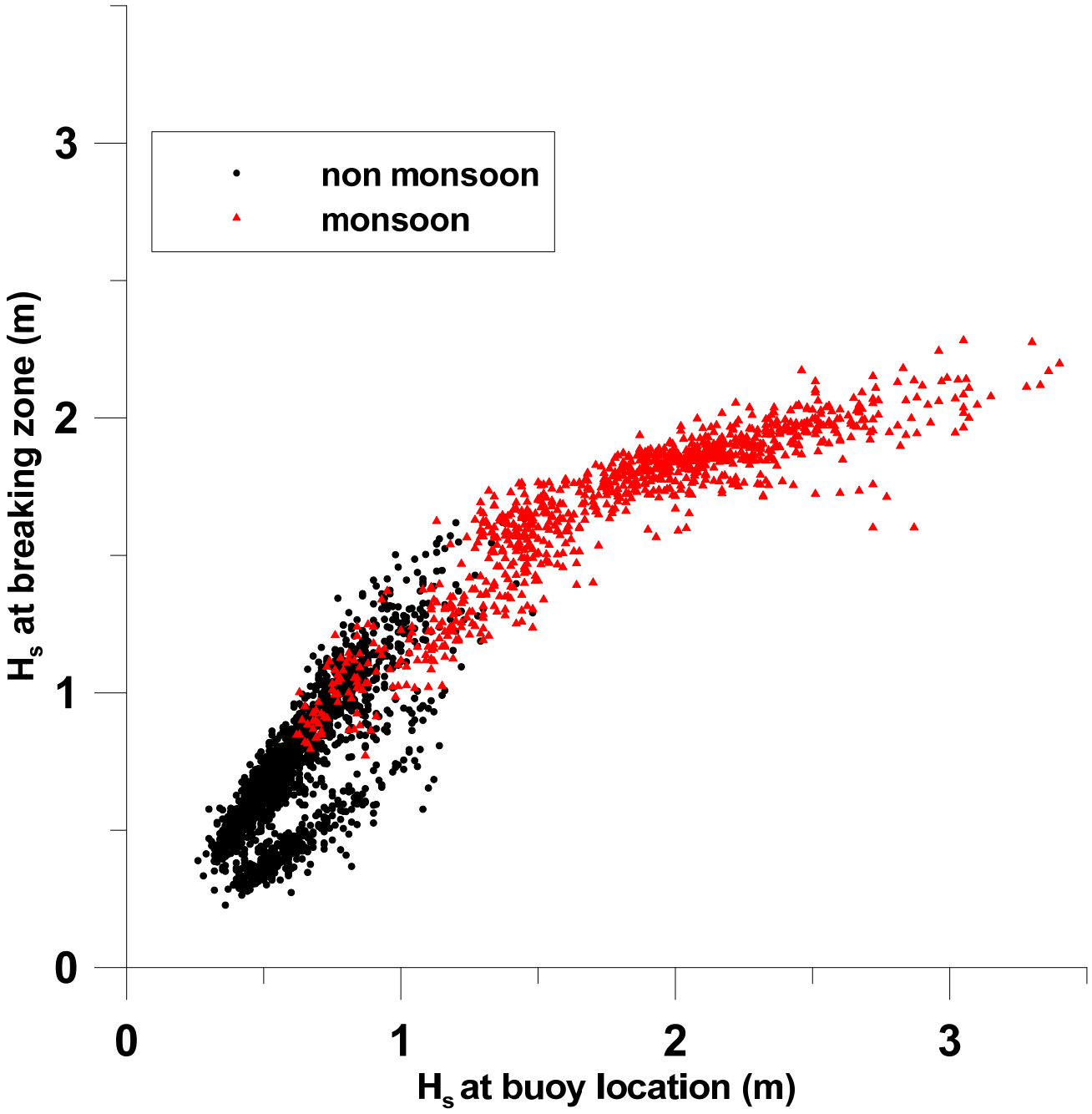

Figure 6.Transformation of significant wave height from 12 m water depth to the breaker zone during monsoon and non-monsoon period. (triangle indicates monsoon and closed circle indicates non-monsoon)

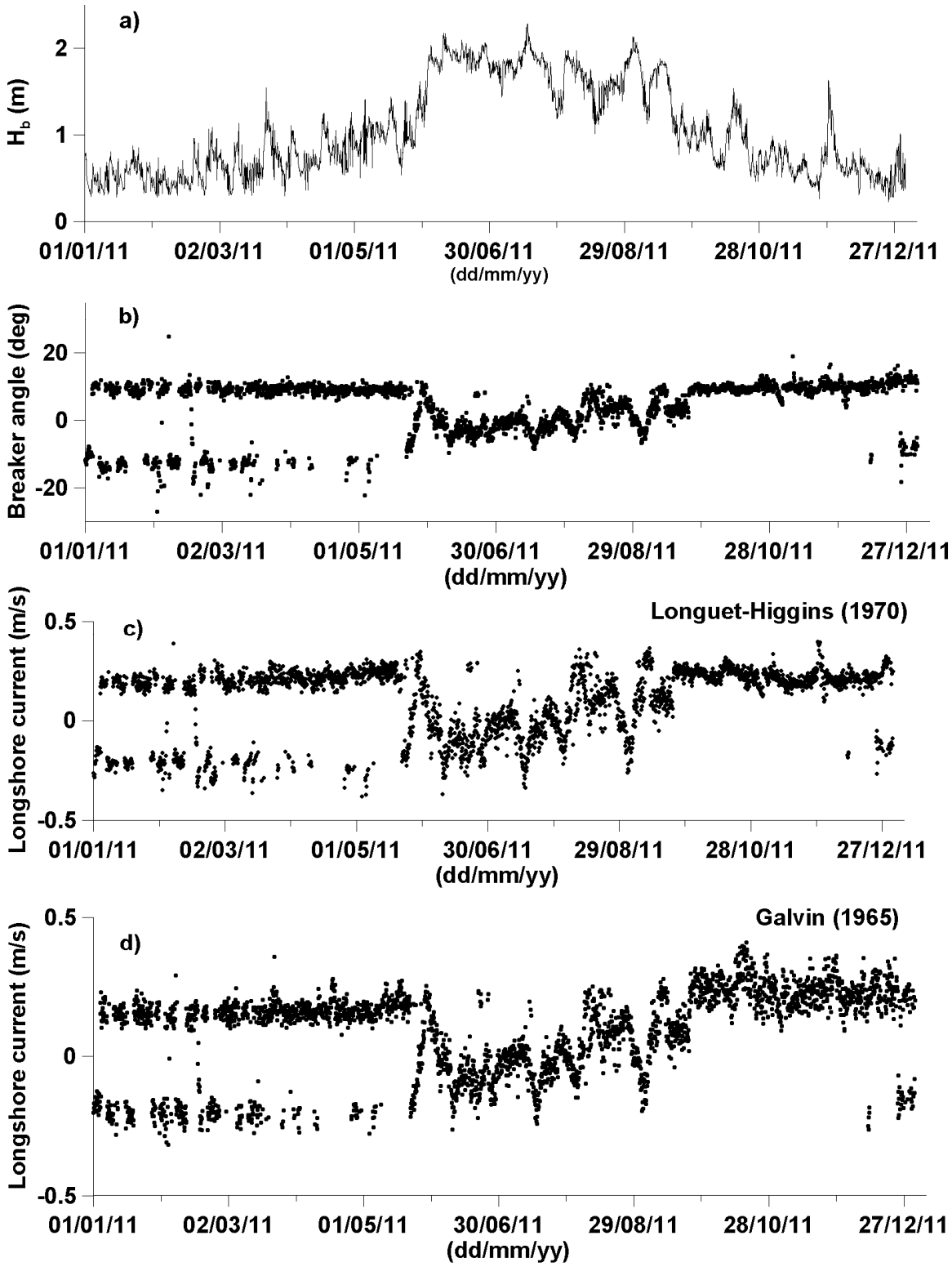

Figure 7. Time-series plot of (a) estimated breaker height, (b) breaker angle, (c) longshore current based on Longuet-Higgins (1970) and (d) longshore current based on Galvin (1965).

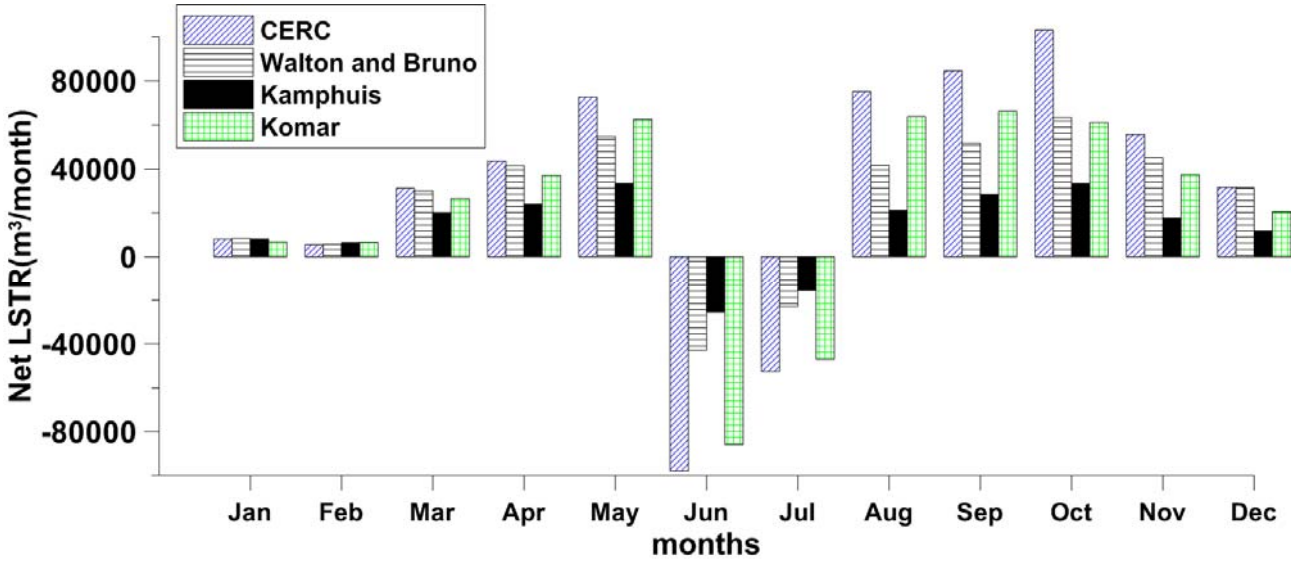

Figure 8. Monthly net longshore sediment transport rate estimated at the breaker zone 1) CERC (forward slash), 2) Walton and Bruno (horizontal lines) 3) Kamphuis (solid) and 4) Komar (cross hatch) formula.

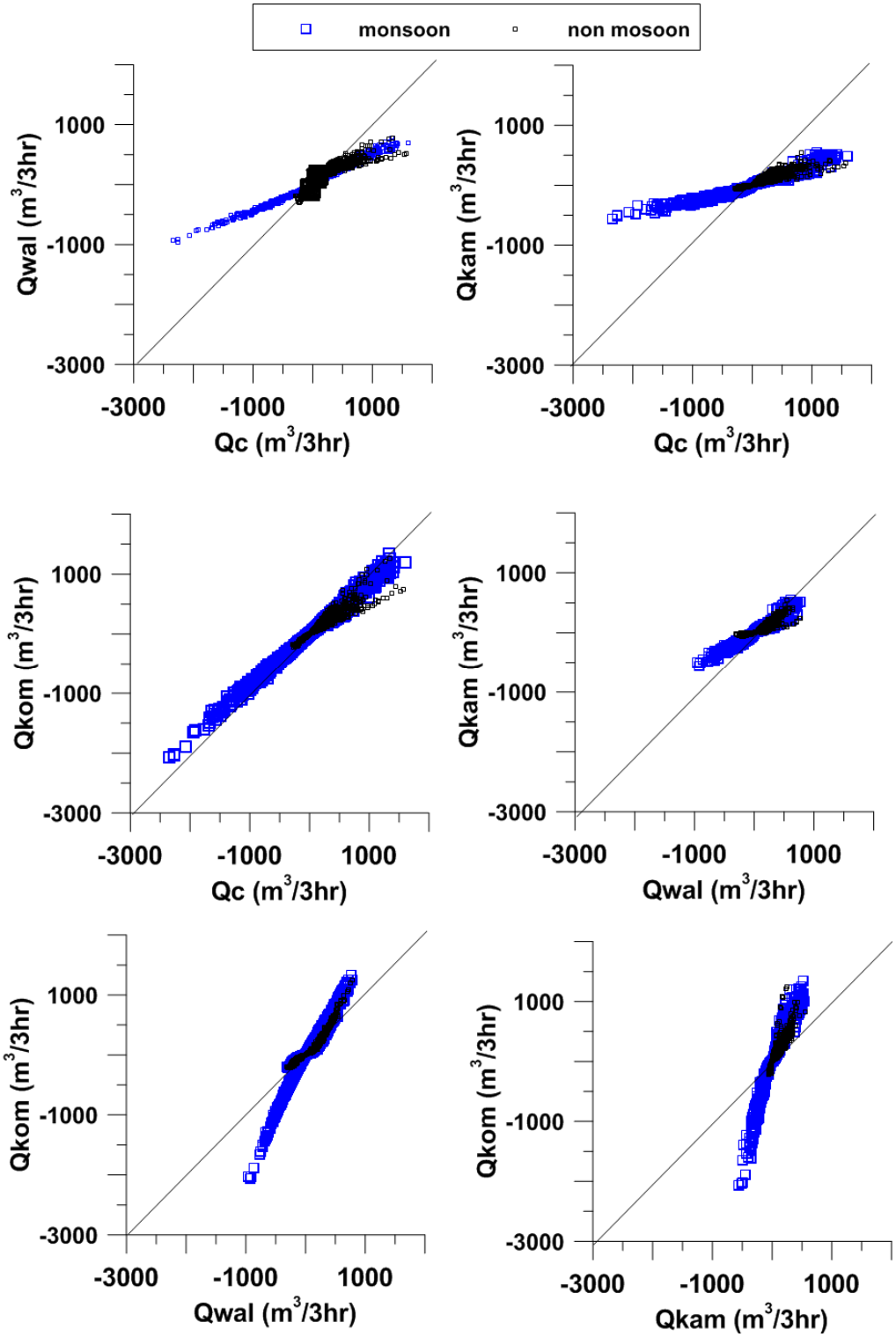

Figure 9. Scatter plots showing comparison of LSTR estimated based on different formulae (Qc-CERC, Qwal-Walton and Bruno, Qkam-Kamphius, Qkom-Komar) (square dot indicates the monsoon and open circle indicates the non-monsoon season)

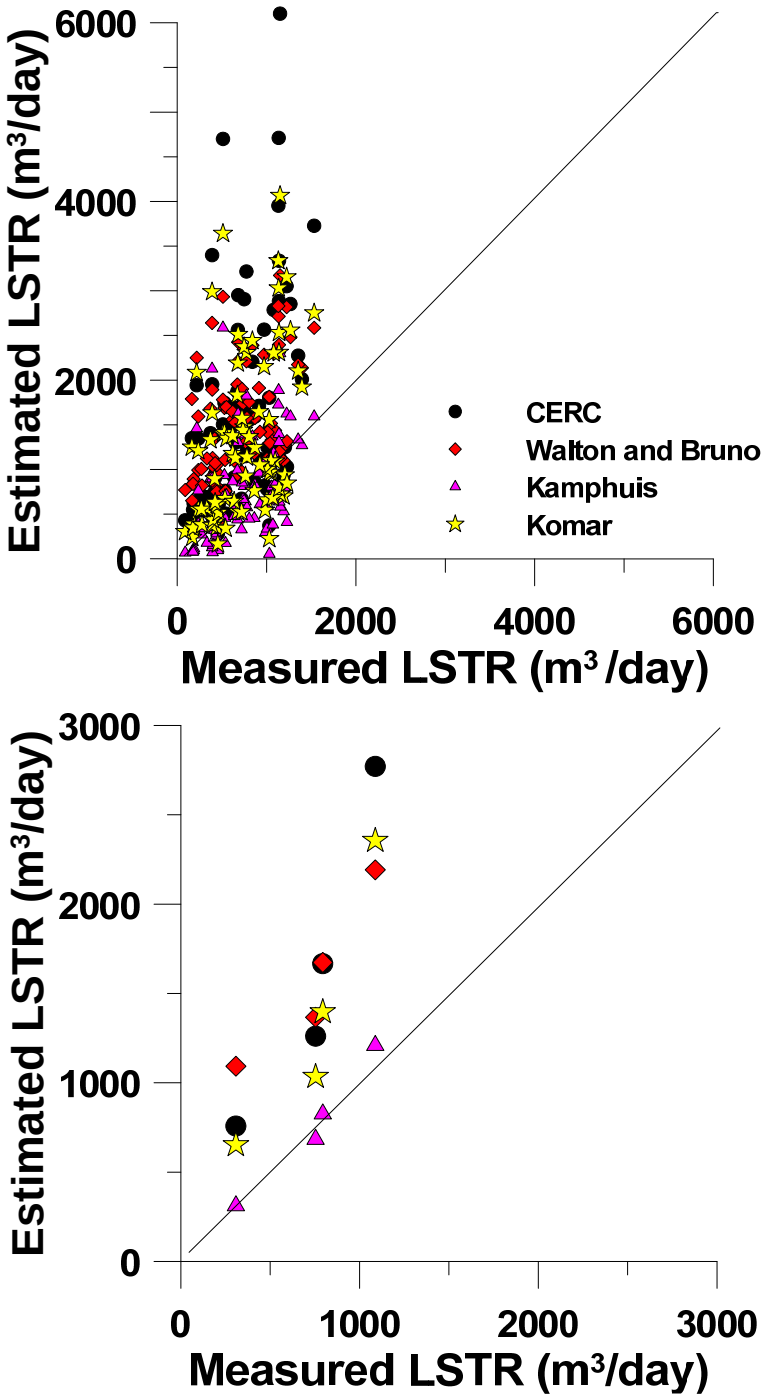

Figure 10. Comparison of estimated LSTR with measured LSTR for (a) daily average and (b) monthly average

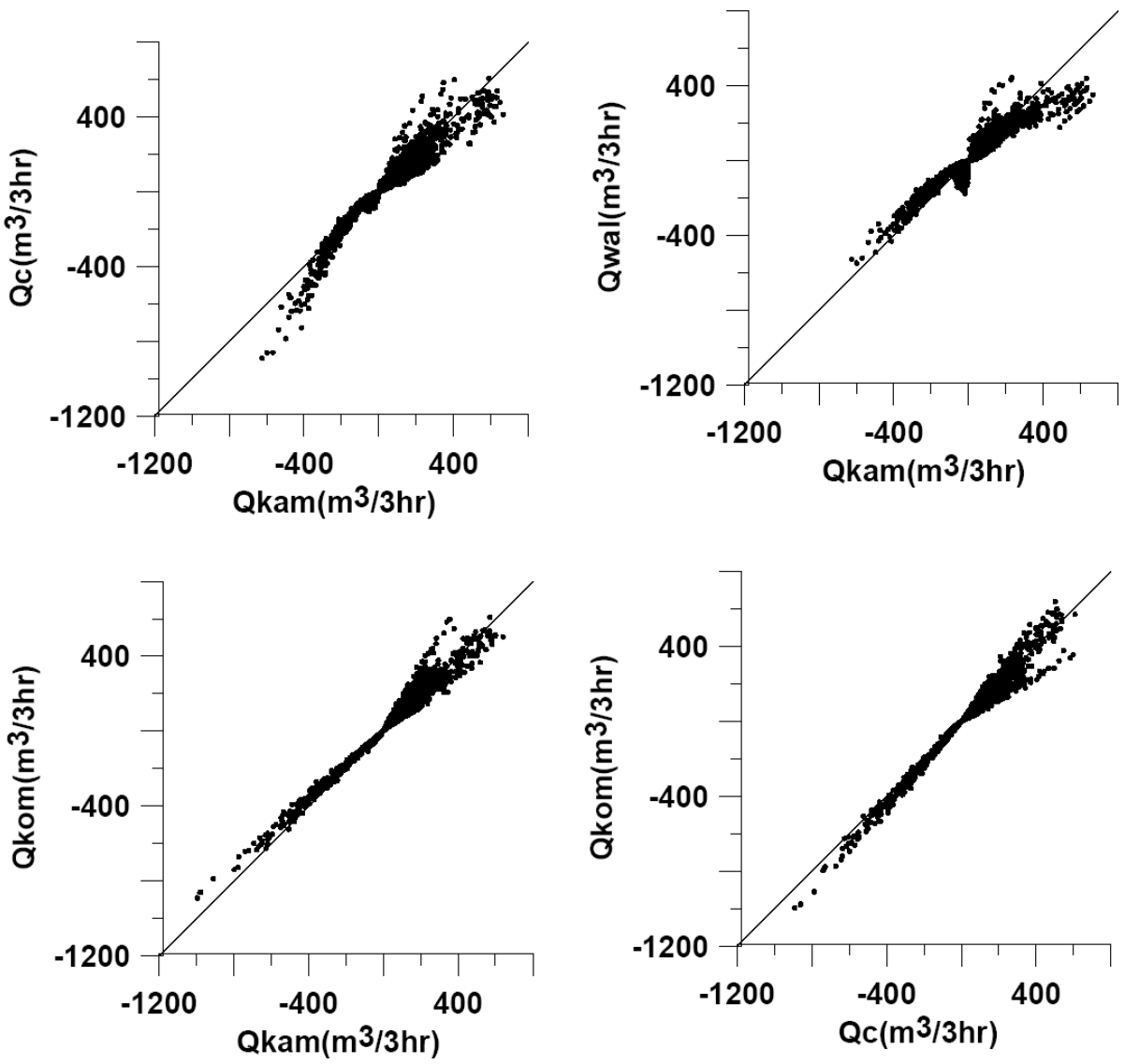

Figure 11. Scatter plots showing comparison of corrected LSTR estimates based on different formulae (Qc-CERC ,Qwal-Walton and Bruno, Qkam-Kamphius, Qkom-Komar)

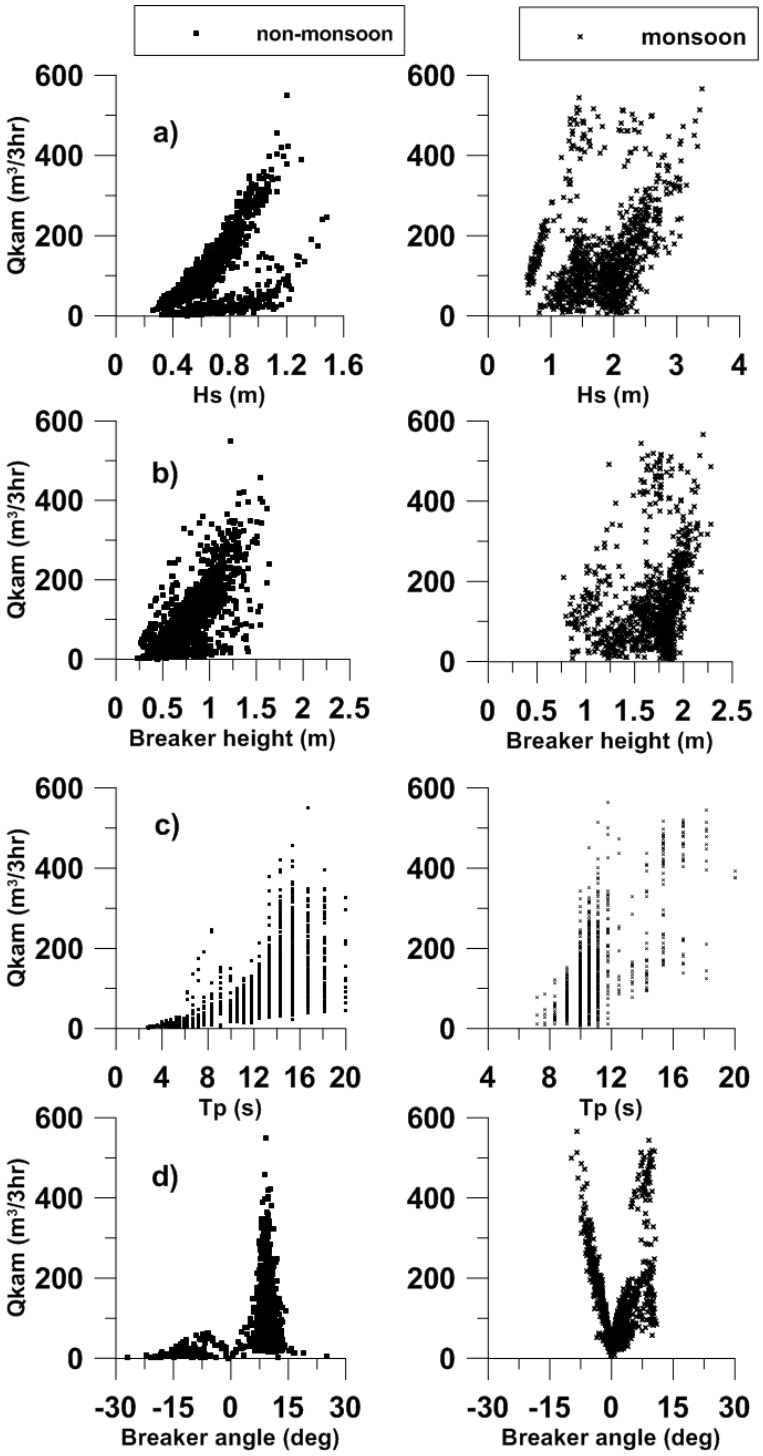

Figure 12. The variation of LSTR based on Kamphuis with a) H_s, b) breaker height, c) Tp and d) breaker angle during non-monsoon (indicated with dots) and monsoon (indicated with cross marks) period.

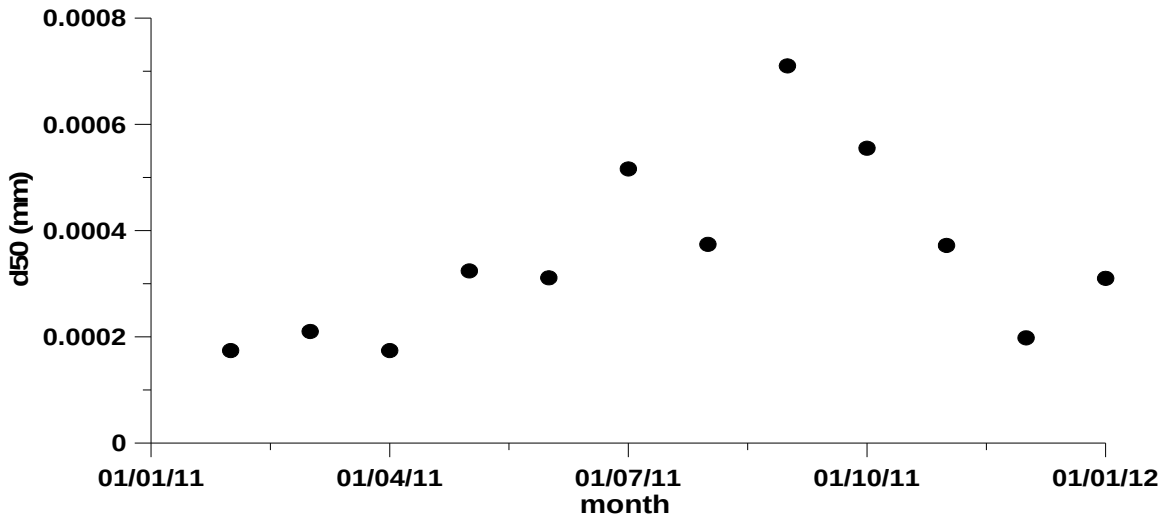

Figure 13. Monthly variation of median grain size (d_{50}) at Kundapura beach.

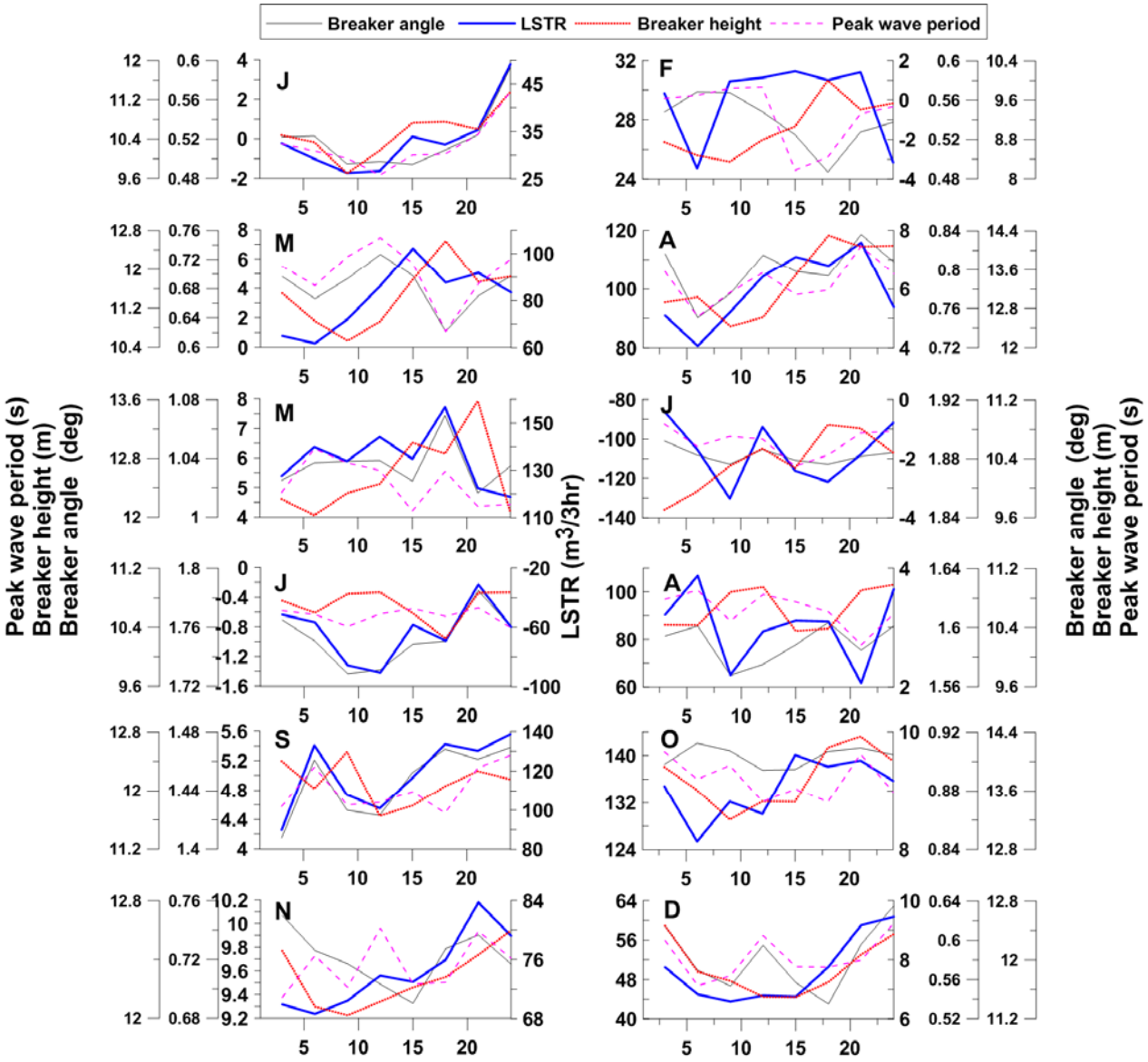

Figure 14. Hourly variation of breaker angle, breaker height, peak wave period and LSTR.

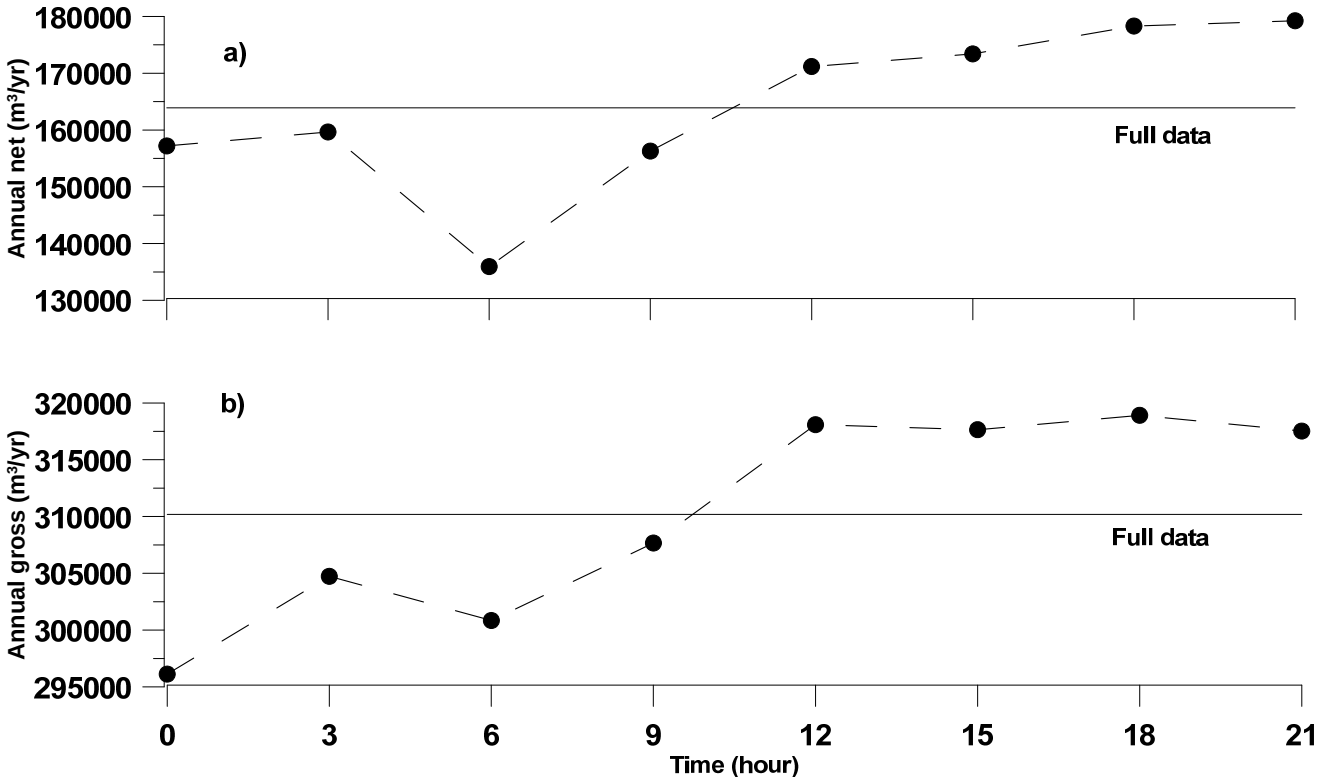

Figire 15. a) Annual net and b) annaul gross LSTR estimate based on data collected at different time of the day and that based on all data.